



Università degli Studi di Cagliari

DOTTORATO DI RICERCA

in

MEDICINA MOLECOLARE E TRASLAZIONALE

Ciclo XXXIII

TITOLO TESI

**Working mechanism of Hic-5 in human and experimental
NAFLD-related liver fibrosis**

Settore scientifico-disciplinare di afferenza

MED/04

Presentata da:

Dott.ssa Simona Onali

Tutor

Prof. Andrea Perra

Co-tutor

Prof.ssa Krista Rombouts

Esame finale anno accademico 2019 – 2020
Tesi discussa nella sessione d'esame Marzo 2021



Simona Onali gratefully acknowledges Sardinian Regional Government for the financial support of her PhD scholarship (P.O.R. Sardegna F.S.E. - Operational Programme of the Autonomous Region of Sardinia, European Social Fund 2014-2020 - Axis III Education and training, Thematic goal 10, Investment Priority 10ii), Specific goal 10.5.

TABLE OF CONTENTS

ABSTRACT	p.4
ABBREVIATIONS	p.8
1. INTRODUCTION	p.10
1.1 NON-ALCOHOLIC FATTY LIVER DISEASE (NAFLD)	p.10
- Definition	p.10
- Epidemiology and risk factors	p.10
- Natural history	p.11
- Pathogenesis	p.12
- Mechanisms of liver fibrogenesis	p.13
1.2 HIC-5 AND ITS ROLE IN LIVER FIBROGENESIS	p.14
1.3 IMPACT OF THYROID HORMONE SIGNALING ON NAFLD AND LIVER FIBROSIS	p.16
2. AIMS	p.17
3. MATERIALS AND METHODS	p.17
3.1 CELL CULTURE	p.17
- Cell treatments using HSC cultured in the traditional 2D model	p.18
- Source of human liver 3D scaffolds	p.18
- Scaffolds preparation	p.18
- Sterilization of human liver 3D scaffolds	p.19
- Repopulation of human liver 3D scaffolds with primary human HSC	p.19
- Cell treatments using HSC cultured in scaffolds	p.19
- Cell viability assay	p.20
- Scaffold collection and storage	p.20
- RNA extraction from HSC	p.20
- Reverse-Transcription for complementary DNA (cDNA) synthesis	p.21
- Quantitative Real-time PCR analysis.	p.21
- Protein extraction from HSC cultured in liver 3D scaffolds	p.22
- Protein quantification	p.22
- Western Blotting	p.22
- Histology	p.23
3.2 ANIMALS	p.24
- Tissue preservation	p.26

- RNA extraction from rat liver samples	p.26
- Gene expression analysis by quantitative Real-time PCR	p.26
- Protein extraction from rat livers	p.27
- Protein quantification	p.27
- Western Blotting	p.27
- Histology	p.28
4. RESULTS	p.30
5. DISCUSSION	p.42
6. REFERENCES	p.45

ABSTRACT

Non-alcoholic fatty liver disease (NAFLD) is characterized by a wide spectrum of pathological findings, ranging from simple steatosis to steatohepatitis which can progress to cirrhosis and hepatocellular carcinoma. Fibrosis severity is the main determinant of liver-related complications and mortality, therefore its regression is considered an important therapeutic endpoint in clinical trials evaluating pharmacological intervention in NAFLD. Activation of hepatic stellate cells (HSC) by transforming growth factor beta (TGF β) is a well-established driver of liver fibrogenesis. Recently, a TGF β -modulated protein, namely hydrogen peroxide-inducible clone 5 (Hic-5) has been proposed as a novel potential therapeutic target for liver fibrosis, since its knockdown attenuated experimental liver fibrosis in mice. However, limited data are available regarding its expression in human HSC, while no study has investigated its role in the setting of NAFLD so far.

Based on these premises, the aim of my thesis was first to characterize Hic-5 expression in human HSC according to different hepatic microenvironment (healthy *versus* fibrotic); secondly to assess whether Hic-5 is expressed in human and experimental NAFLD.

To investigate the first aim, primary human HSC were cultured in a new 3-dimensional (3D) culture model based on decellularized human liver extracellular matrix (ECM) scaffolds derived from healthy and cirrhotic livers. Compared to traditional 2D cultures, Hic-5 gene expression was significantly upregulated in HSC cultured in the 3D model. This effect was further enhanced upon TGF β stimulation in healthy scaffolds. Moreover, higher Hic-5 mRNA levels were detected in HSC cultured in cirrhotic scaffolds compared to healthy scaffolds, suggesting that Hic-5 expression and its modulation by TGF β are strongly affected by liver- and disease specific ECM features.

Based on these preliminary *in-vitro* results, I decided to further investigate Hic-5 expression in human NAFLD samples obtained from obese patients undergoing bariatric surgery. Immunohistochemical staining showed an increased expression of Hic-5 in fibrotic liver tissue, which overlapped alpha smooth muscle actin (α -SMA) positive areas.

In order to better elucidate the role of Hic-5 across NAFLD progression, a nutritional rat model of NAFLD, based on the administration of choline-deficient (CD) diet, was employed and hepatic Hic-5 expression analyzed at different time points. After 3 days of CD diet Hic-5 mRNA levels were not significantly upregulated, suggesting that fatty liver alone without associated liver fibrosis does not affect Hic-5 expression. Accordingly, no difference in α -SMA gene expression was observed compared to control diet. In contrast, administration of CD diet for 7 weeks led to increased mRNA

expression of Hic-5 along with α SMA, TGF β 1 and collagen type 1A1. Upregulation of Hic-5 was further confirmed at the protein level by Western blot analysis. Similar findings were obtained when CD diet was given for 11 weeks. Interestingly, the administration of a triiodothyronine(T3)-supplemented diet for 1 week, which has been previously shown to revert rat fatty liver, was able to reduce the expression of Hic-5. The same effect of T3 on Hic-5 was seen on the microenvironment surrounding preneoplastic nodules during NASH-related experimental liver carcinogenesis. Since T3 administration was associated with regression of preneoplastic nodules not expressing Hic-5 or α SMA, we speculate that its antifibrotic effect may contribute to preneoplastic nodules regression. Taken together, these results highlight the role of Hic-5 in HSC activation in vitro and its association with NAFLD progression. Further studies are needed to clarify the molecular mechanisms regulating Hic-5 expression in NAFLD-related fibrosis and the effects of thyroid receptor's agonists in order to identify potential anti-fibrotic therapies.

ABSTRACT

La steatosi epatica non alcolica (NAFLD) è caratterizzata da un ampio spettro di manifestazioni che spaziano dalla steatosi epatica isolata alla steatoepatite, la quale può evolvere in cirrosi e carcinoma epatocellulare. La gravità della fibrosi epatica è il principale fattore associato alla comparsa di complicazioni della malattia epatica e alla mortalità, pertanto la sua regressione è considerata un importante obiettivo terapeutico negli studi clinici che valutano l'efficacia dei trattamenti farmacologici nei pazienti con NAFLD. L'attivazione delle cellule epatiche stellate (HSC) da parte del transforming growth factor beta (TGF β), è un evento chiave nel processo di fibrogenesi epatica. Recentemente, una proteina modulata dal TGF β , chiamata "hydrogen peroxyde-inducibile clone 5" (Hic-5), è stata proposta come nuovo potenziale target terapeutico per la fibrosi epatica, dal momento che la sua ridotta espressione è stata in grado di ridurre la fibrosi epatica indotta a livello sperimentale nei topi. Tuttavia, esistono dati limitati sulla sua espressione nelle cellule epatiche stellate umane, mentre nessuno studio ha ancora valutato il ruolo di Hic-5 nell'ambito della NAFLD. Sulla base di queste premesse, l'obiettivo della mia tesi è stato dapprima quello di caratterizzare l'espressione di Hic-5 nelle cellule epatiche stellate umane sulla base di differenti microambienti epatici (sano versus fibrotico); in secondo luogo di valutare se Hic-5 fosse espresso nella NAFLD umana e in quella indotta sperimentalmente negli animali.

Per il primo obiettivo, HSC primarie umane sono state coltivate in un nuovo sistema di coltura in 3 dimensioni basato sull'utilizzo di "scaffolds" costituiti da matrice extracellulare (ECM) epatica umana derivata da fegati sani e cirrotici. L'espressione di Hic-5 era significativamente indotta nelle HSC coltivate negli scaffolds rispetto a quelle coltivate nelle tradizionali colture in 2D. Questo effetto era ulteriormente incrementato dall'esposizione al TGF β nelle HSC coltivate negli scaffolds derivati da fegato sano. Inoltre, livelli maggiori di mRNA di Hic-5 sono stati riscontrati nelle HSC coltivate negli scaffolds di fegato cirrotico, suggerendo pertanto che l'espressione di Hic-5 e la sua modulazione da parte del TGF β siano fortemente influenzate da specifiche caratteristiche della ECM epatica. Partendo da questi dati preliminari ottenuti in vitro, ho deciso di studiare ulteriormente l'espressione di Hic-5 in campioni umani di NAFLD ottenuti da pazienti obesi sottoposti a chirurgia bariatrica. Attraverso l'immunoistochimica, si è dimostrata un'aumentata espressione di Hic-5 nel tessuto fibrotico epatico con una marcatura la cui distribuzione è risultata sovrapponibile a quelle delle aree positive per l'alfa smooth muscle actin (α SMA).

Allo scopo di definire meglio il ruolo di Hic-5 nel corso della progressione della NAFLD, ho deciso di utilizzare un modello sperimentale di NAFLD del ratto basato sulla somministrazione di una dieta

colino-deficiente (CD). L'espressione di Hic-5 è stata pertanto analizzata in diversi momenti del suddetto modello sperimentale. Dopo 3 giorni di dieta CD non è stato riscontrato un significativo aumento dei livelli di mRNA di Hic-5, il che suggerisce che la steatosi epatica isolata in assenza di fibrosi non influenzi l'espressione di Hic-5. Allo stesso modo, non è stata osservata alcuna induzione di α SMA rispetto alla dieta di controllo. Al contrario, la somministrazione della dieta CD per 7 settimane ha prodotto un significativo incremento dell'espressione genica di Hic-5, così come anche di α SMA, di TGF β 1 e del collagene di tipo 1A1. L'induzione di Hic-5 è stata inoltre confermata a livello di espressione proteica con l'analisi di Western blotting. Risultati simili sono stati ottenuti quando la dieta CD è stata somministrata per 11 settimane. È interessante sottolineare come la somministrazione di una dieta supplementata con triiodotironina (T3), che si è già dimostrata in grado di indurre una regressione della steatosi epatica nei ratti, abbia ridotto l'espressione genica di Hic-5. Il medesimo effetto della T3 sull'espressione di Hic-5 è stato osservato sul microambiente circostante le lesioni preneoplastiche indotte in un modello sperimentale di cancerogenesi epatica correlata alla NAFLD. Poiché la somministrazione di T3 era associata a regressione dei noduli preneoplastici che non esprimevano Hic-5 o α SMA, abbiamo ipotizzato che il suo effetto antifibrotico abbia potuto contribuire a tale regressione. Ulteriori studi sono necessari per chiarire i meccanismi molecolari che regolano l'espressione di Hic-5 nel contesto della fibrosi epatica associata a NAFLD e per valutare gli effetti degli agonisti dei recettori tiroidei allo scopo di identificare nuove potenziali terapie antifibrotiche.

ABBREVIATIONS

- 3D:** three-dimensional
- α -SMA:** alpha smooth muscle actin
- BDL:** bile duct ligation
- BSA:** bovine serum albumin
- CCl₄:** carbon tetrachloride
- CD:** choline deficient
- COL1A1:** collagen 1-a1
- CS:** choline supplemented
- CTGF:** connective tissue growth factor
- DENA:** diethylnitrosamine
- DIO3:** deiodinase type 3
- ECM:** extracellular matrix
- ELF:** enhanced liver fibrosis
- FBS:** foetal Bovine serum
- FFA:** free fatty acids
- GAPDH:** Glyceraldehyde-3-phosphate dehydrogenase
- GSTP:** glutathione S-transferase placental form
- HCC:** hepatocellular carcinoma
- H₂O₂:** hydrogen peroxide
- HBSS:** Hank's balanced salt solution
- Hic-5:** hydrogen peroxide-inducible clone 5
- HRP:** horseradish peroxidase
- HSC:** hepatic stellate cells
- IMDM:** Iscove's Modified Dulbecco's Medium
- LAP:** latency associated peptide
- LLC:** large latent complexes
- LTBP:** latent trans β binding protein
- LSEC:** liver sinusoidal cells
- NAFLD:** non-alcoholic fatty liver disease
- NAFL:** non-alcoholic fatty liver

NASH: non-alcoholic steatohepatitis

NES: nuclear export signal

PAA: paracetic acid

PBS: phosphate-buffered saline

PDGF: platelet-derived growth factor

PDGFR β : platelet-derived growth factor receptor beta

PNPLA3: patatin-like phospholipase domain-containing protein-3

ROS: reactive oxygen species

RT: Reverse transcription

SLC: small latent complex

SNP: single nucleotide polymorphism

T3: triiodothyronine

TBS-T: Tris-buffered saline with 0.1% Tween[®]20 Detergent

TGF β : transforming growth factor beta

TGF β 111: transforming growth factor beta-1 induced transcript 1

TH: thyroid hormone

THR α : thyroid hormone receptor alfa

THR β : thyroid hormone receptor beta

TSH: thyroid stimulating hormone

VLDL: very-low density lipoprotein

1. INTRODUCTION

1.1 NON-ALCOHOLIC FATTY LIVER DISEASE (NAFLD)

Definition

The term “nonalcoholic fatty liver disease” (NAFLD) refers to a pathological condition characterized by excessive fat accumulation (also known as steatosis) in at least 5% of hepatocytes which occurs in absence of significant alcohol consumption (≥ 30 g/daily for men or ≥ 20 g/daily for women) and alternative causes of fatty liver disease (1).

Two main entities can be distinguished: non-alcoholic fatty liver (NAFL), defined by the presence of isolated hepatic steatosis in the absence of necroinflammation or fibrosis, and non-alcoholic steatohepatitis (NASH), where steatosis is associated to hepatocyte ballooning degeneration and lobular inflammation with or without perisinusoidal fibrosis. While NAFL has been classically considered a benign condition, NASH can potentially progress to cirrhosis, hepatocellular carcinoma (HCC) and end-stage liver disease (2).

Epidemiology and risk factors

NAFLD has recently emerged as a leading cause of chronic liver disease worldwide affecting about 25% of global population. Wide geographical variation across the world has been reported with highest prevalence in the Middle-East, South America and Asia (31.8%, 31.5%, and 27.4%, respectively) and lowest in Africa (13.5%) (3). Epidemiological data on NASH are harder to collect as this condition requires histological confirmation for the diagnosis. However, it is estimated that about 7-30% of NAFLD patients have NASH, which accounts for 1.5-6.5% of worldwide population. According to a recent study, by 2030 the number of NAFLD cases will grow by 18.3%, while NASH prevalence will increase by 15-56%, leading to a subsequent rise in NAFLD-related cirrhosis and mortality (4). NASH is now considered the second most common indication for liver transplantation in United States after chronic hepatitis C, although it is expected to become the most common in the near future (5). Moreover, it will become a dominant cause of HCC in Western countries (6).

NAFLD is classically associated with central obesity, insulin resistance/type 2 diabetes mellitus, hypertension and dyslipidemia, therefore it is considered the hepatic manifestation of the metabolic syndrome (7). Prevalence of NAFLD in obese people is estimated around 91%, while it ranges between 40 to 70% in subjects with type 2 diabetes (8). In addition to these traditional risk factors, a genetic predisposition to NAFLD development has been recently identified in the presence of single nucleotide polymorphisms (SNPs). The best characterized SNP is the allelic variant rs738409 of the patatin-like phospholipase domain-containing protein-3 (PNPLA3) gene located on

chromosome 22q13, which has been associated with increased hepatic fat content, more severe NASH, and an approximately 1.5-fold increased risk of advanced fibrosis or cirrhosis (9,10) as well as HCC (11).

Natural history

The natural history of NAFLD is largely determined by the histopathological features detected at baseline, in particular liver fibrosis stage. Patients showing isolated fatty liver exhibit a low risk of progression to advanced disease with mortality rates similar to that of general population (12). In contrast, finding NASH on liver biopsy is associated with reduced life expectancy from cardiovascular, malignancy or liver-related causes (13). However, it must be noted that recent published studies have challenged this long-standing dogma that NAFL is a benign condition and that NASH is the only prognostically relevant form of the disease. Indeed, some degree of fibrosis progression has been identified also in patients diagnosed with NAFL, although it occurs half as fast as in patients with NASH (approximately one-stage increase in fibrosis every 14 years for NAFL and every 7 years for NASH) (14). Factors associated to fibrosis progression are diabetes mellitus, severe insulin resistance, high body mass index, weight gain greater than 5 kg, cigarette smoking, systemic hypertension and rising transaminase levels. Overall, the rate of progression to cirrhosis over a 15-year period is estimated around 11%, although rates of fibrosis progression are quite variable among patients (15). A rapid evolution to advanced fibrosis is observed in around 20% of patients (the so-called rapid progressors), while the remaining 80% shows little or no worsening of fibrosis (slow progressors) (Fig.1). Once reached the cirrhotic stage, decompensation occurs in about 31% of patients over a 8-year period, whereas HCC development is estimated around 7% in 6.5 years of follow-up. Risk factors for HCC in NASH include age, obesity, diabetes, iron deposition and the PNPLA3 I148M polymorphism. Finally, a major concern is the potential for HCC to arise in a non-cirrhotic NASH, which has been documented in up to 50% of cases, especially in the presence of the metabolic syndrome. These tumours are frequently diagnosed at a more advanced stage than in patients with viral hepatitis, possibly due to insufficient surveillance, which may contribute to the poorer prognosis observed in several studies (16–18).

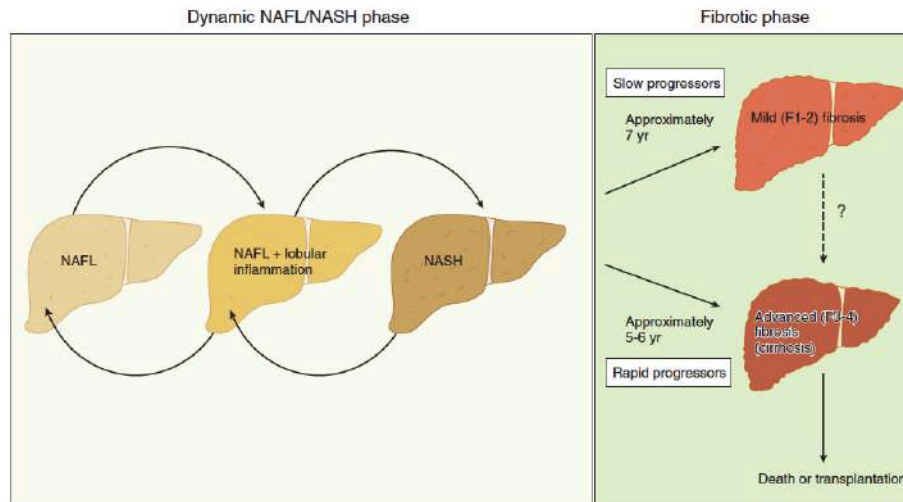


Figure.1 The dynamic model of NAFLD (from Zakim and Boyer's Hepatology: A Textbook of Liver Disease, 7th ed)

Pathogenesis

The pathogenesis of NAFLD development and progression is complex and multifactorial. In 1988 Day and colleagues proposed the so-called “two hit hypothesis” which postulated that in the setting of steatosis (first hit), a “second hit” from other factors (such as oxidative stress) was required for NASH development (19). However, it became rapidly evident that this view was too oversimplified to describe human NAFLD, where multiple factors act synergistically in genetically predisposed subjects in a complex crosstalk between different organs and tissues, such as adipose tissue, pancreas, gut and liver. Therefore, a multiple-hit model has now replaced the outdated two-hit hypothesis (20). Briefly, dietary habits, environmental and genetic factors can lead to insulin resistance, obesity and changes in gut microbiome. Dysregulated insulin signaling results in increased hepatic de novo lipogenesis and adipose tissue lipolysis, which produce an enhanced flux of free fatty acids (FFA) to the liver. Normally, FFAs undergo mitochondrial beta oxidation or are further converted to triglycerides to be exported into the blood as VLDL (very-low density lipoprotein) or stored in lipid droplets. When the liver capacity to handle FFA influx is overwhelmed, lipotoxic species accumulate in the hepatocytes inducing endoplasmic reticulum stress, production of reactive oxygen species (ROS) and multiple inflammatory pathways (21). Furthermore, insulin resistance also promotes the production and release of adipokines and inflammatory cytokines, which further contribute to hepatocyte damage (22). In addition to that, perturbation of gut microbiome impairs the intestinal barrier function with increased permeability, endotoxemia and low grade inflammation (23). Altogether, these factors are responsible for hepatocyte injury and

death, which ultimately lead to hepatic macrophage (Kupffer cells) and hepatic stellate cell (HSC) activation and subsequent inflammation and fibrosis (Fig.2).

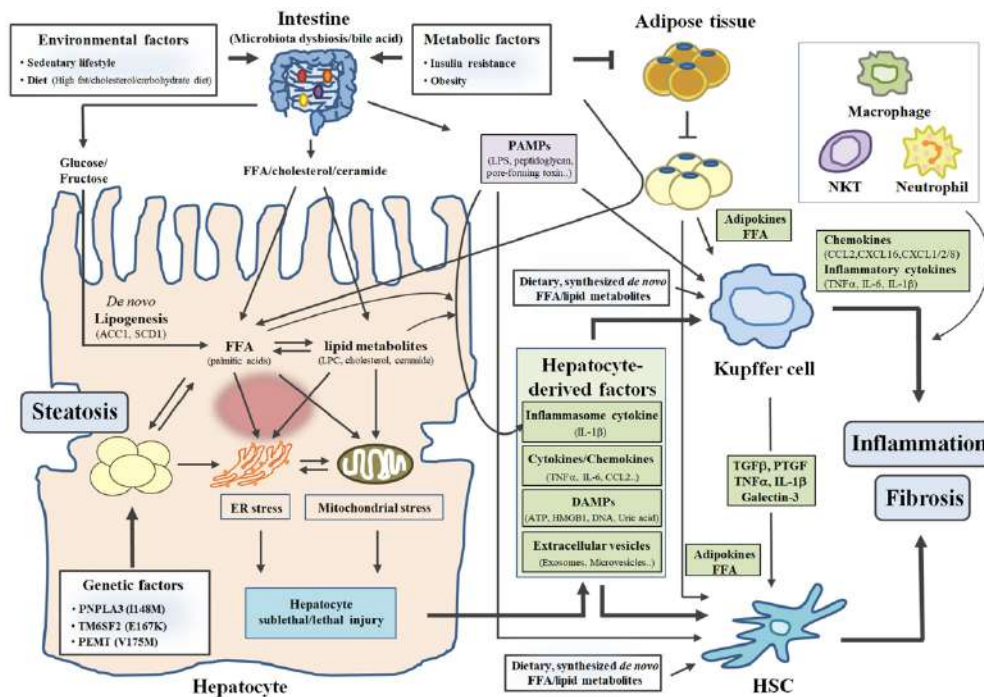


Figure 2. Multiple parallel-hit model in NAFLD pathogenesis (24)

Mechanisms of liver fibrogenesis

The severity of liver fibrosis is the main determinant of mortality in patients with NASH (25,26). Liver fibrosis is the result of an excessive ECM production that is not counterbalanced by adequate degradation, thus resulting in net accumulation. In addition to increased amounts, the composition of the ECM also changes in fibrosis with increased crosslinks that make ECM more resistant to degradation. Modifications in ECM induce liver sinusoidal cells (LSEC) to lose fenestra and to form a basement membrane in a process called sinusoidal capillarization (27). This phenomenon interferes with normal nutrient transport between sinusoidal cells and surrounding cells, especially hepatocytes, causing functional disturbance and profound architectural distortion, which eventually lead to cirrhosis and liver failure.

Hepatic stellate cells (HSC) represent the main determinant of hepatic fibrosis contributing to 80-95% of collagen-producing myofibroblasts in different mouse model of fibrosis, including NASH (28). Under physiological conditions, HSC reside in the space of Disse, in close contact with hepatocytes and sinusoidal endothelial cells, exhibiting a quiescent phenotype. Morphologically they have a star-like shape and are characterized by the presence of cytoplasmic lipid droplets containing vitamin A as retinyl palmitate (29). Signaling from stressed/injured hepatocytes and Kupffer cells leads to

activation of HSC into myofibroblasts, which lose the retinoid storage capacity while exhibiting increased proliferation and contractility. Activated HSC show a greater expression of pericellular matrix proteins, such as alpha-smooth muscle actin (α -SMA) and vimentin, and secrete abundant extracellular proteins, including fibronectin and collagen type I and III.

In cooperation with other pathways triggered by ROS, platelet-derived growth factor (PDGF) and connective tissue growth factor (CTGF), transforming growth factor-beta 1 (TGF β) signaling is considered the most potent fibrogenic pathway that drives HSC activation and ECM deposition (29). Quiescent HSC only express a minimum amount of TGF β , which is upregulated shortly after liver injury. Besides HSC, additional hepatic sources of TGF β are LSEC, macrophages and hepatocytes (30). TGF β is initially synthesized as a pre-pro-TGF β protein which undergoes homodimerization in the rough endoplasmic reticulum to form the pro-TGF β . This homodimer is cleaved by furin-like proteases to generate C-terminal mature peptides and N-terminal LAP (latency associated peptide) which constitute the so-called small latent complex (SLC). SLC is then secreted from the cell into the ECM where SLC can covalently bind to latent TGF β binding protein (LTBP) to form a large latent complex (LLC) (31). Release of active TGF β from ECM is determined by multiple factors, including high or low pH, cleavage by specific proteases (i.e. metalloproteinases) or interactions with integrins, such as integrin α V expressed by HSC (32).

Binding to TGF β receptors I and II triggers the activation of multiple intracellular signaling pathways which mediate the profibrogenic effects of TGF β . One of the best studied pathways is the so-called canonical SMAD-dependent pathway, characterized by the phosphorylation of SMAD2 and SMAD3, their association to SMAD4 and translocation into the nucleus to bind DNA and regulate the transcription of pro-fibrogenic target genes. This pathway is tightly regulated by inhibitory SMAD proteins (SMAD6 and SMAD7), which can be induced by TGF β as a negative feedback loop.

1.2 HIC-5 AND ITS ROLE IN LIVER FIBROGENESIS

TGF β signaling modulatory proteins have gained a growing interest in order to identify potential therapeutic targets for liver fibrosis. Recently a TGF β modulated protein, namely hydrogen peroxide-inducible clone 5 (Hic-5), has been shown to interfere with TGF β /SMAD2 signaling in HSC, while its deficiency has been associated with attenuation of liver fibrosis in mice through upregulation of SMAD7 (33).

Hic-5, also known as transforming growth factor beta-1 induced transcript 1 (TGF β 111), has been originally identified as a gene induced by hydrogen peroxide (H₂O₂) and TGF β , encoding a focal

adhesion protein with homology to paxillin (34). It is strongly expressed by smooth muscle cells at different sites, including large intestine, uterus, ovary, bronchial airways and blood vessels (35). High expression is detected in mesenchymal cells lines, while its expression is generally low in epithelial cell lines.

In the cytoplasm Hic-5 localizes at focal adhesion sites, which are complex multi-protein structures that mediate interactions between cells and ECM, thereby coordinating cell mobility, survival and proliferation in response to adhesion status (36). In response to mechanical stress Hic-5 can translocate from focal adhesions to actin stress fibers, thus regulating cell contractile capability.

Moreover, this protein can shuttle between focal adhesions and the nucleus via an oxidant-sensitive nuclear export signal (NES), participating in the transcriptional regulation of several genes (i.e. p21, c-Fos) and operating as a co-activator of steroid receptors, such as progesterone, androgen and glucocorticoid receptor (37).

Regarding its role in fibrogenesis, Hic-5 has been found to upregulate TGF β signaling through its ability to directly interact with SMAD7 in a myofibroblast cell line (38) and to promote scar formation by regulating the TGF β autocrine loop in hypertrophic scar myofibroblasts (39). In a rat model of glomerulosclerosis Hic-5 expression in glomeruli was markedly increased and was associated with a strong induction of type 1 collagen and apoptotic cells, suggesting a crucial impact of Hic-5 in glomerulosclerosis (40). Moreover, recent studies have highlighted the role of Hic-5 in intestinal and pancreatic fibrosis (41,42). Furthermore, increased Hic-5 expression has been observed in dermal fibroblasts derived from patients affected by systemic sclerosis, while its mRNA knockdown was able to reduce collagen 1 production in the same cells, further supporting the concept that Hic-5 could represent a novel target for future antifibrotic therapies (43).

In normal liver Hic-5 has been detected only in the vascular smooth muscle cells of Glisson's sheath, whereas an enhanced expression has been observed in fibrotic human livers, where Hic-5 distribution overlaps with α -SMA positive HSC. In mouse fibrotic livers generated by bile duct ligation (BDL) or carbon tetrachloride (CCl₄) injection of Hic-5 was highly expressed only in HSC, but not in LSEC, Kupffer cells and hepatocytes. Conversely, Hic-5 KO mice subjected to BDL or CCl₄ administration showed a significant decrease in fibrosis compared to wild-type animals, with a marked downregulation of collagen 1 and III gene expression and reduced protein levels of α -SMA. Moreover, Hic-5 deficiency was associated with enhanced SMAD7 protein levels in murine and human HSC, indicating that Hic-5 could modulate TGF β /SMAD2 signaling interfering with its inhibitory feedback loop (33).

Finally, Hic-5 has recently been shown to be abundant in decellularized human cirrhotic liver scaffolds compared to healthy liver scaffolds using label-free proteomic analysis proteomics (44).

1.3 IMPACT OF THYROID HORMONE SIGNALING ON NAFLD AND LIVER FIBROSIS

Triiodothyronine (T3), the active form of thyroid hormone (TH), plays a critical role in maintaining metabolic homeostasis throughout life, regulating de novo lipogenesis, fatty acid oxidation, cholesterol and carbohydrate metabolism (45). A meta-analysis including 15 observational studies reported a significant association between hypothyroidism and increased risk of NAFLD, independently of age, sex, body mass index and other common metabolic risk factors (46). Conversely, NAFLD patients were found to have significantly higher levels of thyroid stimulating hormone (TSH) compared to healthy controls, as well as a greater prevalence of overt hypothyroidism (47). More interestingly, recent findings suggest that, independently of systemic TH levels, NAFLD is associated with a local hepatic hypothyroidism characterized by impaired T3 action in the liver. Expression of thyroid hormone-responsive genes was found to be inversely correlated with liver fat in obese patients and to be similarly decreased in mice with obesity induced by high-fat feeding (48). In the liver of patients with NAFLD an increased expression of the T3-inactivating enzyme deiodinase type 3 (DIO3) was detected (49), as well as a reduced expression of thyroid hormone receptor beta (THR β), the main form of TH receptor which mediates the genomic actions of T3 in the liver (50). Moreover, complete regression of liver steatosis has been observed in a nutritional rat model of NASH after administration of a T3-supplemented diet for 1 week (51).

Since systemic thyroid therapy cannot be proposed as a therapeutic strategy for NAFLD, several selective THR β agonists have been developed to optimize the beneficial effects on the liver while minimizing the detrimental effects on heart and bone that are mainly mediated by THR alpha (THR α). Among these new compounds, MGL-3106 (also called Resmetirom) and VK2809 have recently been shown to strongly reduce hepatic fat content in patients with NASH, further supporting the use of T3 analogs as a therapeutic strategy for NAFLD (52,53). However, no significant improvement in liver fibrosis was noted in patients treated with Resmetirom, although there was a reduction in non-invasive fibrosis markers including enhanced liver fibrosis (ELF) and N-terminal type III collagen pro-peptide.

Based on these background, further studies are needed to better define the impact of T3 signaling in the liver, focusing not only on its well-established metabolic effects but also investigating its influence on liver fibrosis. Indeed, controversial results exist in the literature regarding the role of

T3 on HSC activation and liver fibrogenesis, since both pro-fibrogenic and anti-fibrogenic effects have been reported (54–57).

2. AIMS

Based on the published data regarding the role of Hic-5 in liver fibrogenesis together with my own observations that Hic-5 is up-regulated in decellularized human cirrhotic scaffolds compared to healthy scaffolds, the aims of the present project are to:

1. Characterize Hic-5 expression and its modulation by pro-fibrogenic stimuli in human hepatic stellate cells cultured in human healthy and cirrhotic ECM liver scaffolds.
2. Investigate whether Hic-5 is expressed in human NAFLD.
3. Analyze Hic-5 expression across NAFLD progression employing a nutritional rat model of NAFLD able to recapitulate the different stages of the disease.
4. Investigate the effects of thyroid hormone on liver related fibrosis and Hic-5 expression in a rat model of NAFLD

3. MATERIAL AND METHODS

3.1 CELL CULTURE

Primary human HSC were isolated from wedge sections of human liver tissue, obtained from patients undergoing liver surgery at the Royal Free Hospital after giving informed consent (NC2015.020 (B-ERC-RF)), as previously described (58,59). Cells derived from a single donor were used for the experiments. HSC were expanded until the desired amount of cells was obtained and used until passage 8.

Cells were grown in Iscove's Modified Dulbecco's Medium (IMDM) supplemented with 20% Foetal Bovine serum (FBS), 1% sodium pyruvate, 1% non-essential amino acids, 1% glutamine and 1% penicillin/streptomycin/amphotericin B. Cells were incubated at controlled humidity and temperature (37°C) with 5 % CO₂. Complete culture medium was changed every 72 hours. When passaging cells, medium was removed and cells were washed twice with Hank's balanced salt solution (HBSS). The trypsin-EDTA solution was added with a volume depending on the size of the culture flask, usually 4 ml for a T175 flask. After 2-3 minutes incubation, cell detachment was verified under microscope and complete culture medium (usually 6 ml for a T175 flask) was added to inactivate trypsin. The cell suspension was collected by pipetting up and down with serological pipettes several times and mixed thoroughly. Cells were then centrifuged at 1600 rpm for 6 minutes

and supernatant was discarded. Afterwards, cells were re-seeded in new flasks containing the complete medium (an average of 10^6 cells in 20ml medium for a T175 flask).

The medium, HBSS and trypsin-EDTA were stored at +4°C refrigerator. FBS stock solutions were stored at -20°C refrigerators. All solutions and media were warmed at 37°C water bath prior to use. Cell count was performed using a disposable plastic haemocytometer.

Cell treatments using HSC cultured in the traditional 2D model

Primary human HSC were seeded in Petri dishes and maintained in complete culture medium, which was changed every 72 hours. At day 10 HSC were treated with TGF β 5 ng/ml for 24 hours. Next, cells were washed twice with sterile PBS 1x and then frozen at -80°C for further analysis.

Source of human liver 3D scaffolds

3D scaffolds, or acellular liver tissue cubes, were derived from healthy or cirrhotic human livers. Both the organs were obtained under the UCL Royal Free BioBank Ethical Review Committee approval (NRES Rec Reference: 11/WA/0077). Informed consent was obtained for each donor and confirmed via the NHSBT ODT organ retrieval pathway. Two different livers were used to prepare the cubes: one was an organ discarded for transplant without histological evidence of fibrosis and fat accumulation, while the other one was an explant from an alcoholic cirrhotic patient.

Livers were first perfused with 1% phosphate-buffered saline (PBS, Sigma-Aldrich, UK) to eliminate blood and then frozen at -80°C for a minimum of 24h. Afterwards, human livers were thawed at 4°C overnight, cut into 125 mm³ cubes and stored again at -80°C for future use.

Scaffolds preparation

The decellularization protocols to obtain 3D scaffolds from human liver tissue cubes were established at the Institute for Liver and Digestive Health, Regenerative Medicine and Fibrosis (WO2015185912 A1 and WO2017017474), University College London, UK (44,60). Liver cubes were first placed in 2 mL tubes and thawed in a 37 °C water bath for 45 min followed by incubation for 15 min with the addition of 1.5 mL of PBS 1X (from Sigma-Aldrich). Afterwards, cubes were transferred in decellularization solution and placed in QIAGEN TissueLyser II and frequency of oscillation was set at 30 Hz. Tissue decellularization was achieved by multiple cycles of agitation in decellularization solutions such as deionized water (Milli-Q[®] ultrapure water, VWR, Leicestershire, UK), reagent mixture (detergents and enzyme), and PBS1X. The same concentrations were used for

both healthy and cirrhotic liver tissue, although protocols were optimized according to each tissue and cycles were repeated according to the saturations of detergents (44).

Sterilization of human liver 3D scaffolds

After decellularization, scaffolds were sterilized using a solution containing 0.1% paracetic acid (PAA) (Sigma) and 4% absolute ethanol for 30 minutes in an orbital shaker (Staurt). Afterwards, the sterilizing solution was changed and cubes were incubated again for other 15 minutes. Two washing steps were performed using sterile 1X HBSS (Thermofisher Scientific) for a total of 30 minutes in an orbital shaker. The sterile scaffolds were then placed in a 48 well plate for 24 hours in the incubator (37°C and 5% CO₂) with complete culture medium to assess the sterilization method prior to the addition of the cells.

Repopulation of human liver 3D scaffolds with primary human HSC

Before cell seeding, the sterilized scaffolds were transferred into a 96 well plate. HSC cultures were trypsinised, as already described, and resuspended at a concentration of 0.3×10^6 cells in 20 μ L. Scaffolds were repopulated with cells using the drop-on technique (60) and placed in the incubator on an orbital shaker to enhance engraftment. After 30 minutes, the cells were collected from the bottom of each well and reseeded on the top to increase cell engraftment. This step was repeated 3 times. Afterwards, 140ul of complete culture medium was added to each scaffold and the plate was placed in the incubator at 37°C with gentle agitation overnight. The following day scaffolds were transferred in a 48-well plate and 1.4 ml of complete culture medium added to each well. Medium was changed every 72 hours.

Cell treatments using HSC cultured in scaffolds

All treatments were performed at day 10 from cell seeding.

Experimental procedure 1: HSC cultured in healthy scaffolds (n=4 per condition) were exposed to increased H₂O₂ concentrations (10-50-100 μ M, Sigma Aldrich) for 24 hours.

Experimental procedure 2: HSC cultured in parallel on plastic Petri dishes and in healthy scaffolds (n=4) were exposed to TGF β 1 (5ng/ml, R&D SYSTEMS) for 24 hours.

Experimental procedure 3: primary human HSC grown in both healthy and cirrhotic scaffolds (n=4 per condition) were treated in serum-free medium as follows: (1) H₂O₂ (100 μ M) for 24 h; (2) TGF β 1 (5 ng/mL,) for 24 hours; (3) H₂O₂ 100 μ M and TGF β 1 5ng/ml simultaneously for 24 hours; (4) H₂O₂

100 μ M or TGF β 1 5ng/ml pre-treatment for 6 hours followed by simultaneous treatment with H₂O₂ 100 μ M and TGF β 1 5ng/ml for 18 hours.

Cell viability assay

Culture medium was discarded and the scaffolds were incubated in Presto Blue solution (ThermoFisher Scientific) diluted 1:10 in culture medium. The cells were exposed to Presto blue in the dark for 2.5 hours in a humidified incubator at 37°C with 5% CO₂.

Fluorescence was read immediately after incubation on a Fluostar Omega fluorescence microplate reader (BMG Labtech) and quantified using excitation and emission wavelengths of 540 nm and 595 nm. The data measured in arbitrary units for the treated samples were normalized to the negative control (non-treated samples) and expressed as percentages (%).

Scaffold collection and storage

One scaffold per group was collected, fixed in 4% formaldehyde for 24 hours and then processed using the Leica TP1020 automated tissue processor. Processing included dehydration in 70%, 80%, 95%, 100% ethanol, followed by clearing xylene treatment and inclusion in paraffin.

The remaining scaffolds were snap-frozen in liquid nitrogen and stored at -80°C for further analysis.

RNA extraction from HSC

Total RNA was extracted from 3D cultures using Qiazol Lysis Reagent (Qiagen) and RNeasy Plus Universal Kit (Qiagen) as described by the manufacturer's instruction and as previously published (60). Each frozen scaffold was placed in a 2 mL tubes with a 5 mm stainless steel bead (Qiagen), 900 μ L of Qiazol Lysis Reagent and homogenised by shaking at 30 Hz for 2 to 4 minutes on TissueLyser II. The content of the tube (excluding the bead) was then transferred to a new 1.5 ml centrifuge tube and RNA extracted following the manufacturer's protocol.

For 2D samples 900ul of Qiazol Lysis was added to each well and a cell scraper was used to detach the cells from the plastic.

After extraction, RNA concentrations and purity ratios (260/280 and 260/230) were measured using NanoDrop 1000 Spectrophotometer (Thermo Scientific).

Reverse-Transcription for complementary DNA (cDNA) synthesis

Reverse transcription (RT) from mRNA to cDNA was performed using the High Capacity cDNA Reverse Transcription Kit (Applied Biosystems), as described by the manufacturer's instructions. Briefly, the RNA samples were diluted in order to obtain a concentration not lower than 10 ng/ μ l, and 10 μ l of each sample was added in a PCR microtube. Subsequently, 10 μ l of the 2X RT mastermix was added to each tube to have a final volume of 20 μ l.

The RT mastermix contained: 2 μ l of RT buffer (10X), 2 μ l of Random Primers (10X), 0.8 μ l of dNTP mix (100 mM), 1 μ l of MultiScribe™ Reverse Transcriptase, 1 μ l of RNase Inhibitor and 3.2 μ l of DNase/RNase-free distilled water.

Thermo cycle condition was: 25° C for 10 minutes, 37° C for 120 minutes and 85° C for 5 minutes, followed by a 4° C hold. Samples were then stored at -20° C until next use.

Quantitative Real-Time PCR analysis

Gene expression was measured using TaqMan gene expression assays with the Applied Biosystems® 7500 Real-Time PCR system. The cDNA was diluted in order to have a concentration of 1 ng/ μ L. A qPCR Master Mix was prepared following manufacturer's instruction.

Specific TaqMan Probes for the different human target genes were used (Applied Biosystems, listed in Table 1). cDNA (5 μ l) was added together with 15 μ l of the qPCR Mastermix in a Fast Optical 96-well TaqMan PCR plate (MicroAmp Applied biosystems). The microplate was then inserted in a 7500 Fast Real Time PCR System (Applied Biosystems®). Expression levels for each gene were calculated using the delta Ct method and normalized to the Ct of Glyceraldehyde-3-phosphate dehydrogenase (GAPDH) as reference gene, as previously described (58).

Gene	Assay ID	Dye:	Company
GAPDH	Hs02786624_g1	FAM	Thermo Fisher
TGFB111	Hs00210887_m1	FAM	Thermo Fisher
ACTA2	Hs00426835_m1	FAM	Thermo Fisher
COL1A1	Hs00164004_m1	FAM	Thermo Fisher
TGFB1	Hs00998133_m1	FAM	Thermo Fisher

Table 1. List of TaqMan gene expression assay used in HSC

Protein extraction from HSC cultured in liver 3D scaffolds

Healthy and cirrhotic scaffolds were washed in PBS 1X for 5 minutes, and then each sample lysed in a 2 ml centrifuge tube containing a 5 mm steel bead and 200 μ L of RIPA buffer (Sigma Aldrich) completed with 10 μ L protease and phosphatase inhibitors (Roche), 10 μ L PMSF, 5 μ L of NaF, and 5 μ L of Na₃VO. Tissue disruption was obtained using the TissueLyser II (Qiagen) at 30Hz for 4 minutes. Samples were then put on ice followed by centrifugation at 4°C for 10 minutes at 14000 rpm. The supernatant was collected and stored at -80°C until further use.

Protein quantification

Protein quantification was performed using the MicroBCA protein assay kit (Thermo Fisher Scientific). Lysates were diluted 1:100 in ultra-pure water and then incubated in a 96-well plate for 2 hours at 37°C with the MicroBCA reagents, as indicated in manufacturer's instructions. Each sample was analyzed in duplicate. Absorbance was measured at 562nm using a Fluostar Omega microplate reader.

Western Blotting

Protein lysates (15 μ g) were prepared by adding Laemmli Sample buffer (4X LDS, Bio-rad) and 5% β -Mercaptoethanol and boiled for 5 minutes at 95°C, to achieve protein denaturation.

Protein lysates were run onto a SurePAGE gel (Bis-Tris 4-12%, Genscript) at 140V for 1.5 hour in the Running Buffer (Tris-MOPS-SDS, Genscript). After the run, gels were assembled in a "sandwich"-like structure with the following order from top to bottom: cathode (-), fiber pad, filter paper, gel, transfer membrane, filter paper, fiber pad, anode (+). In this way, the negatively charged proteins were transferred into the PVDF membrane (Immobilon-P, Millipore) by using Transfer Buffer (Genscript) at 100V for 1 hour. Ponceau S was used to stain the protein bands on the membranes in order to check the transfer and equal loading. Membranes were washed with ultra-pure water and then incubated for one hour with 5% of bovine serum albumin (BSA) in TBS-T in order to avoid nonspecific binding sites.

To detect specific proteins, the membranes were incubated over-night at 4 ° C with the indicated primary antibody diluted in 5% BSA in TBS-T (Table 2). The immunoreactivity was detected by incubation for one hour at room temperature with secondary antibody conjugated to HRP (Horseradish Peroxidase) followed by enhanced chemiluminescence reaction (SuperSignal™ West Pico PLUS Chemiluminescent Substrate, Thermo Scientific) and exposure on the FluorChem Western

Blot Scanner (Protein simple). Blots were stripped by incubation for 10 minutes at room temperature with Stripping buffer (Thermo Fisher) and incubated with GAPDH antibody diluted in %5 BSA in TBS-T as an internal control and equal loading.

Primary Antibody	Species	Dilution	kDa	Company and catalogue number	Secondary Antibody
Hic-5	mouse	1:250	50	BD Bioscience 611165	SantaCruz
Alfa-SMA	mouse	1:5000	42	Sigma A2547	m-IgGκ BP-HRP
GAPDH	mouse	1:200	37	SantaCruz sc 47724	Sc 516102 1:10,000

Table 2. Antibodies used for Western Blotting and IHC for HSC cultured in 3D scaffolds

Histology

Haematoxylin and Eosin staining

Paraffin embedded scaffolds were sliced into 4 µm sections using a Leica RM2035 microtome (Leica biosystems). All sections were dewaxed using xylene and rehydrated. After hydration, sections were treated with Harris' haematoxylin (Leica biosystems) for 10 minutes and then washed in tap water for 10 minutes. The sections were checked under the microscope and, when necessary, quickly washed in 0.5% acid-alcohol for a few seconds in order to obtain an adequate differentiation between ECM and cell nuclei. Next, the sections were stained with eosin (Leica biosystems) for 4 minutes, followed by washing with water. Subsequently, the sections were dehydrated with ethanol for few seconds and then soaked in xylene for 10 minutes before mounting.

Immunohistochemical stainings

Details regarding the immunohistochemistry protocols are reported in Table 3. Briefly, after dewaxing and hydration, the sections were washed in TBS-T for 5 minutes. Heat-induced antigen retrieval was performed soaking the sections in a pre-warmed retrieval solution (Citrate Buffer pH 6.0) which was heated in a microwave at medium potency. Next, peroxide blocking solution (3%) was used for 5 minutes to inhibit endogenous peroxidase activity and then, after washing with TBS-T, blocking serum (normal horse serum 2.5%, ABC Kit Vector) was added for 5 minutes. Sections were incubated with the primary antibody at different conditions, depending on the antibody used (Table 3). After washing with TBS-T for 5 minutes, incubation with a-ready-to-use secondary biotinylated antibody (VECTASTAIN Elite ABC HRP Kit Peroxidase, Universal, and R.T.U.) was

performed for 30 minutes at room temperature. Slides were then washed again and placed for 30 minutes in ABC complex (VECTASTAIN Elite ABC HRP Kit Peroxidase, Universal, and R.T.U.) and 3,3'-Diaminobenzidine (DAB, Novolink 7230-K Leica) was used as chromogen for 5 minutes. Slides were finally counterstained with Harris Haematoxylin (Sigma-Aldrich) for 1 minute, dehydrated through graded alcohols and cleared. Coverslips were mounted with synthetic mounting medium.

Antigen	Retrieval	Primary antibody	Dilution	Incubation
Hic-5	20 min	BD Bioscience (BD 611165)	1:100	Overnight at 4°C
PDGFR β	10 min	Abcam (Ab32570)	1:50	1 hour at room temperature
Ki67	20 min	Abcam (Ab21700)	Pre-diluted	1 hour at room temperature

Table 3. Details of immunohistochemistry protocols for HSC cultured in 3D scaffolds

3.2 ANIMALS

F344 and Wistar male rats were purchased from Charles River (Milan, Italy). On arrival, the animals were fed a rodent standard diet (Standard diet 4RF21, Mucedola, Milan, Italy) and water at libitum, with alternating 12-hour dark-light cycle and acclimatized to laboratory conditions for 1 week before the start of experimental procedures. Standard room temperature and humidity were kept through the entire period of experimentation. Animals were maintained in accordance with the Guidelines of the Animal Ethics Committee of the University of Cagliari and all procedures were authorized by the Italian Ministry of Health.

Experiment 1

Four adult male Wistar rats (150 g of weight) received 2 weekly subcutaneous injection of carbon tetrachloride (CCl₄) for 9 weeks. Each animal received 2 ml of CCl₄ (50% v/v in corn oil), or the same volume of the vehicle (control group). Animals received standard laboratory diet throughout the experiment. Animals were culled after 3 days from the last injection of CCl₄ (Fig.2A).

Experiment 2

Seven four-week old male F344 rats were fed a Choline Deficient (CD) diet (Mucedola, Milan), prepared according to the formula used in Lombardi's group (62), for 3 days and then sacrificed. A separate group of 7 animals received a control diet, which was identical to the CD diet but supplemented with a normal amount of choline (CS diet) (Fig.2B).

Experiment 3

Twenty four-week old male F344 rats were divided into 4 groups as follows: group 1 (n=5) was fed a CS diet for 7 weeks; group 2 (n=5) was a fed a CD for 7 weeks; group 3 (n=5) received a CD diet for 6 weeks and then was fed a CD diet containing 4mg/kg T3 for 1 week; group 4 (n=5) was fed a CD diet for 6 weeks and subsequently a CS for a week. At the end of the 7th week all animals were sacrificed (Fig.2C).

Experiment 4

Ten five-week old male F344 rats were initiated with a single intraperitoneal dose of diethylnitrosamine (DENa, Sigma-Aldrich), dissolved in saline, at a dose of 150 mg/Kg body weight. Following a 2-week recovery period, all rats were fed the CD diet for 10 weeks. Then the animals were divided into 2 groups: one group was maintained on a CD diet for an extra week, while the other was fed a CD diet containing 4 mg/kg T3 for 1 week and then sacrificed (Fig.2D).

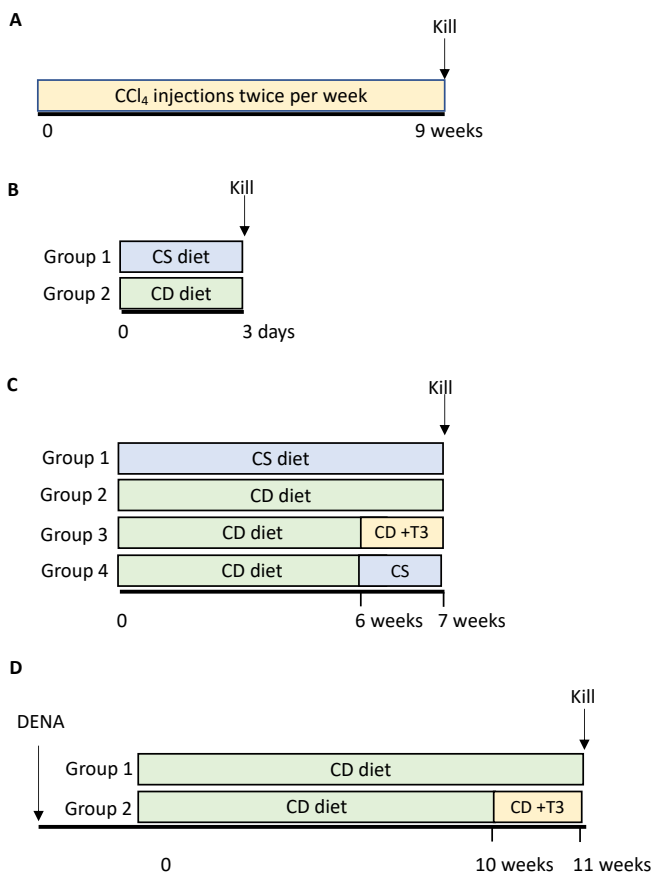


Figure 2. Animal experimental protocols. CCl₄: carbon tetrachloride; CS: choline supplemented; CD: choline deficient; DENa: diethylnitrosamine; T3: triiodothyronine.

Tissue preservation

Immediately after sacrifice, liver was harvested and the different lobes were separated. Four 3 mm thick sections were cut from each of the main lobes, two of which were fixed in 10% buffered formalin and the other two were quickly snap frozen in liquid nitrogen cooled isopentane. Frozen samples were preserved at -80°C for future molecular analysis and formalin fixed tissue were embedded in paraffin and stored at room temperature.

RNA extraction from rat liver samples

Total RNA extraction was performed using the miRNeasy Mini Kit (Qiagen) according to manufacturer's protocol. Briefly, 700 µl of Qiazol Lysis Reagent (Qiagen) was added to each liver sample in a 2 ml tube and tissue was disrupted and homogenized using a Tissue Ruptor (Qiagen) for 30 seconds. After 5-minutes incubation at room temperature, 140 µl of chloroform was added and each tube was shaken vigorously for 15 seconds. Samples were then centrifuged for 15 minutes at 4°C to obtain the separation of the aqueous phase containing the RNA, which was subsequently collected in a new collection tube and processed as indicated by the instructions.

Extracted RNA concentrations and purity ratios (260/280 and 260/230) were measured using NanoDrop 1000 Spectrophotometer (Thermo Scientific).

Gene expression analysis by quantitative Real-time PCR

In order to analyse the mRNA levels of different target genes, total RNA was retrotranscribed to cDNA using the High Capacity cDNA Reverse Transcription Kit (4374966, Applied Biosystem, Life Technologies, Italy), as already described.

Once cDNA was obtained, the amplification reaction was performed in a final volume of 10 µl containing 4 µl of cDNA template (2.5 ng/µl), 5 µl of 2X TaqMan Gene Expression Master Mix (Applied Biosystem, Life Technologies), 0.5 µl of 20X TaqMan assay (Applied Biosystem, Life Technologies, Table 4) and 0.5 µl of RNase-free water. Gapdh was used as endogenous control. To determine the relative expression level, the $2^{-\Delta\Delta CT}$ method was used.

Gene	Assay ID	Dye:	Company
Gapdh	Rn99999916_s1	FAM	Thermo Fisher
Tgfb1I1	Rn01511346_g1	FAM	Thermo Fisher
Acta2	Rn01759928_g1	FAM	Thermo Fisher
Tgfb1	Rn00572010_m1	FAM	Thermo Fisher
Col1a1	Rn01463848_m1	FAM	Thermo Fisher

Table 4. List of Taqman rat gene expression assays

Protein extraction from rat livers

Protein extraction was performed adding 1 ml of RIPA buffer completed with the Halt protease and phosphatase inhibitors cocktail (Sigma 78440) at 1:100 dilution. Tissue was homogenized using the Tissue ruptor (Qiagen) and then incubated in ice for 30 minutes. Next, samples were centrifuged at 4°C for 15 minutes twice and supernatants were collected and stored at -80°C until further use.

Protein quantification

Protein lysates were mixed with 125 µl of Reagent A (Bio-Rad DC Protein Assay, #5000113) and 1 ml of Reagent B (Bio-Rad DC Protein Assay, #5000114). A standard BSA curve was generated as a reference for protein quantification. Each sample was then incubated for 15 minutes at room temperature. Absorbance was read at 750nm using a spectrophotometer.

Western blotting

Protein lysates (70µg) were mixed with RIPA buffer and sample buffer (NuPage Invitrogen NP0008 4X) and denaturated at 70°C for 10 minutes in a thermoblocker. Next, samples were separated by PAGE using a pre-cast gel (NuPage 4-12% Bis-Tris, Invitrogen) and MOPS-SDS as running buffer (NuPage 0001, Invitrogen) applying 120V for 1h and 45 minutes. After run, the gel was assembled in a “sandwich”-like structure with the following order from top to bottom: cathode (-), 2 fiber pads, filter paper, gel, transfer membrane, filter paper, 2 fiber pads, anode (+). Protein were transferred to the transfer nitrocellulose membrane (Bio-Rad, cat 1620097) by using Transfer Buffer (NuPage Transfer Buffer 20X + Methanol 20% in distilled water) at 30V for 1 hour. Ponceau S was used to stain the protein bands on the membranes in order to check the transfer. Membranes were washed with distilled water and then incubated for one hour with 5% of BSA in TBS-T in order to avoid

nonspecific binding sites. Further details regarding the primary and secondary antibodies used are reported in table 5.

Primary Antibody	Species	Dilution	kDa	Company and catalogue number	Secondary Antibody
Hic-5	mouse	1:250	50	BD Bioscience 611165	Santa Cruz m-IgGκ BP-HRP, Sc 516102 1:4000
Alfa-SMA	mouse	1:2000	42	Abcam Ab7817	
GAPDH	rabbit	1:10,000	37	Synaptic system 247002	Cell Signaling Anti-rabbit IgG, #7074 1:5000

Table 5. *Antibodies used for Western Blotting for protein extracted from rat livers*

Histology

Haematoxylin and Eosin staining

Four micron thick liver sections were mounted on positive charged microscope glass slides and heated at 60°C for 10 minutes, cleared in xylene and rehydrated with serial ethanol dilutions. Sections were incubated for 20 minutes with ready-to-use Carazzi's Haematoxylin (Bio-Optica), washed in tap water and then stained with 1% aqueous Eosin Y (Bio-Optica) for 20 seconds. After several rinses in tap water, the sections were dehydrated through ascending alcohol dilutions, cleared with xylene and covered with synthetic mounting medium (Bio-Optica) and coverslips.

PicroSirius Red staining

After standard dewaxing and rehydration protocol, 4µm thick rat liver sections were incubated with Picro-sirius Red solution (Direct Red 80, Sigma Aldrich, dissolved in saturated aqueous solution of picric acid 1.2%) for 1 hour. Next, samples were quickly washed in two changes of acidified water containing 0.5% acetic acid, then dehydrated and covered with mounting medium and coverslips.

Immunohistochemistry

Four micron thick liver sections were deparaffinized through heating at 60°C for 10 minutes and soaking in xylene for 1 hour. Next, sections were rehydrated as previously described.

For anti-GSTP staining, sections were incubated in 0.5% H₂O₂ (Sigma Aldrich) in distilled water for 10 minutes to block endogenous peroxidase activity. After two washes in PBS, blocking of unspecific binding sites was performed in 10% normal goat serum (Abcam, ab7481) for 30 minutes at room

temperature in a humid chamber. Sections were then incubated overnight with 1:1000 diluted anti-GSTP antibody (MBL 311) at 4°C in a humidified chamber. Next day, slides were washed twice in PBS and then incubated with anti-rabbit HRP-linked secondary antibody (Sigma A045) at 1:300 dilution in PBS for 30 minutes at room temperature. Positive binding reaction was visualized using VECTOR NovaRED Peroxidase Substrate kit (Vector Laboratories) for 4 minutes at RT. Afterwards, slides were counterstained with Harris Haematoxylin (Sigma), dehydrated and cleared in xylene before mounting the coverslips.

For anti-Hic-5 and α -SMA staining, after dewaxing and rehydration the protocol included a step for antigen retrieval which was achieved soaking the slides in a pre-warmed Citrate buffer solution (Antigen retrieval buffer, Abcam 93678) which was heated at 750 W in a microwave. After cooling down, slides were washed in TBS and incubated in 0.5% H₂O₂ (Sigma Aldrich) in distilled water for 10 minutes. After washing in TBS, incubation with primary antibodies was performed overnight at 4°C in a humidified chamber (Table 6). Next day the slides were washed twice with TBS and incubated with a-ready-to-use anti-mouse secondary antibody (DAKO EnVision + system, HRP-labelled polymer, K4001) for 45 minutes at room temperature. DAB (Vector Laboratories) was used as chromogen and Harris haematoxylin for counterstaining, as already described.

Antigen	Retrieval time	Primary antibody	Primary antibody dilution	Incubation
GSTP	Not needed	MBL311	1:1000	Overnight at 4°C
Hic-5	30 min	BD 611165	1:100	Overnight at 4°C
Alfa-SMA	20 min	Abcam (Ab 7817)	1:1000	Overnight at 4°C

Table 6. Summary of primary antibodies used for IHC staining of rat liver samples.

4. RESULTS

Hic-5 gene expression in primary human HSC cultured in 3D scaffolds: effect of TGF β and hydrogen peroxide exposure.

The first set of experiments was performed by re-seeding decellularized healthy human liver scaffolds with primary human HSC (0.3×10^6). Cells were able to populate not only the surface but also the core of the scaffolds, showing their characteristic elongated protrusions (Fig.3).

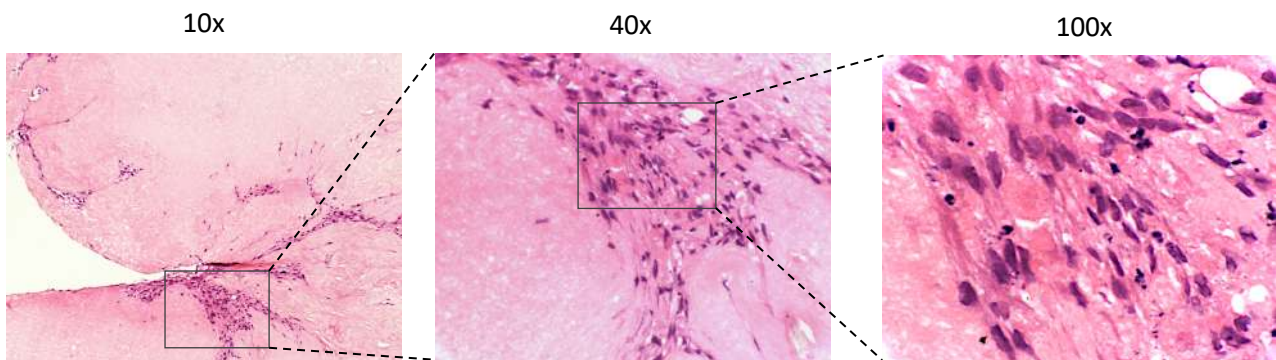


Figure 3. Representative images of haematoxylin and eosin-stained sections of primary human HSC engrafting the healthy human liver scaffolds for 11 days (10x, 40X and 100X magnification).

To investigate whether Hic-5 was differentially expressed by primary human HSC cultured in 3D scaffolds compared to the traditional plastic cultures, cells were cultured in Petri dishes and in healthy liver scaffolds up to 10 days and then exposed to TGF β 5ng/ml for 24 hours. Already in basal conditions, comparative gene expression analysis by qRT-PCR showed a significant upregulation of Hic-5 in HSC cultured in the 3D model in comparison to 2D cell cultures, suggesting a specific ECM-induced effect. Upon TGF β treatment, Hic-5 mRNA levels were further increased only in the 3D model (Fig.4).

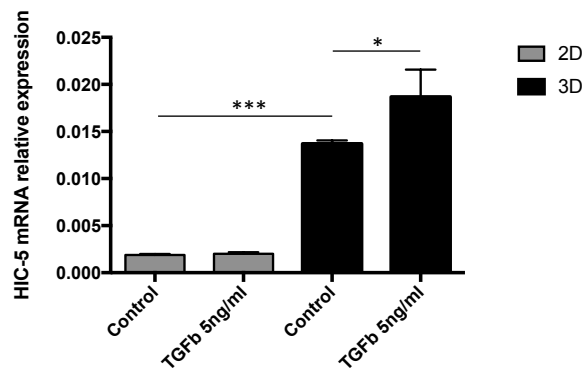


Figure 4. Upregulation of Hic-5 gene expression in HSC cultured in healthy liver scaffolds compared to 2D cultures. Relative mRNA expression level assessed by qRT-PCR; GAPDH was used as endogenous control. N=4 per condition tested; each bar represent mean \pm standard deviation. * $p < 0.05$; *** $p < 0.001$ one-way ANOVA

The second step was to elucidate whether hydrogen peroxide could also affect Hic-5 expression in human HSC, as previously published studies have demonstrated that Hic-5 expression is induced by H₂O₂. Therefore, HSC were seeded in healthy liver scaffolds and cultured in complete medium up to day 10, followed by exposure to increasing concentrations of H₂O₂ (10-50-100 μM) for 24 hours. Histological examination of the scaffolds demonstrated that cell engraftment and proliferation was preserved upon H₂O₂ exposure, as shown by haematoxylin and eosin staining and by PDGFβ-receptor and Ki67 immunohistochemistry, respectively (Fig.5A-C). Indeed, several Ki-67 positive nuclei could be observed, as well as numerous PDGFβ-receptor positive stained cells. Gene expression analysis by qRT-PCR showed an upregulation of Hic-5 mRNA levels after the treatment with H₂O₂ 50μM and 100 μM (Fig.5D). Taken together, these preliminary findings suggest that both TGFβ and H₂O₂ affect Hic-5 expression in human HSC cultured in healthy liver scaffolds.

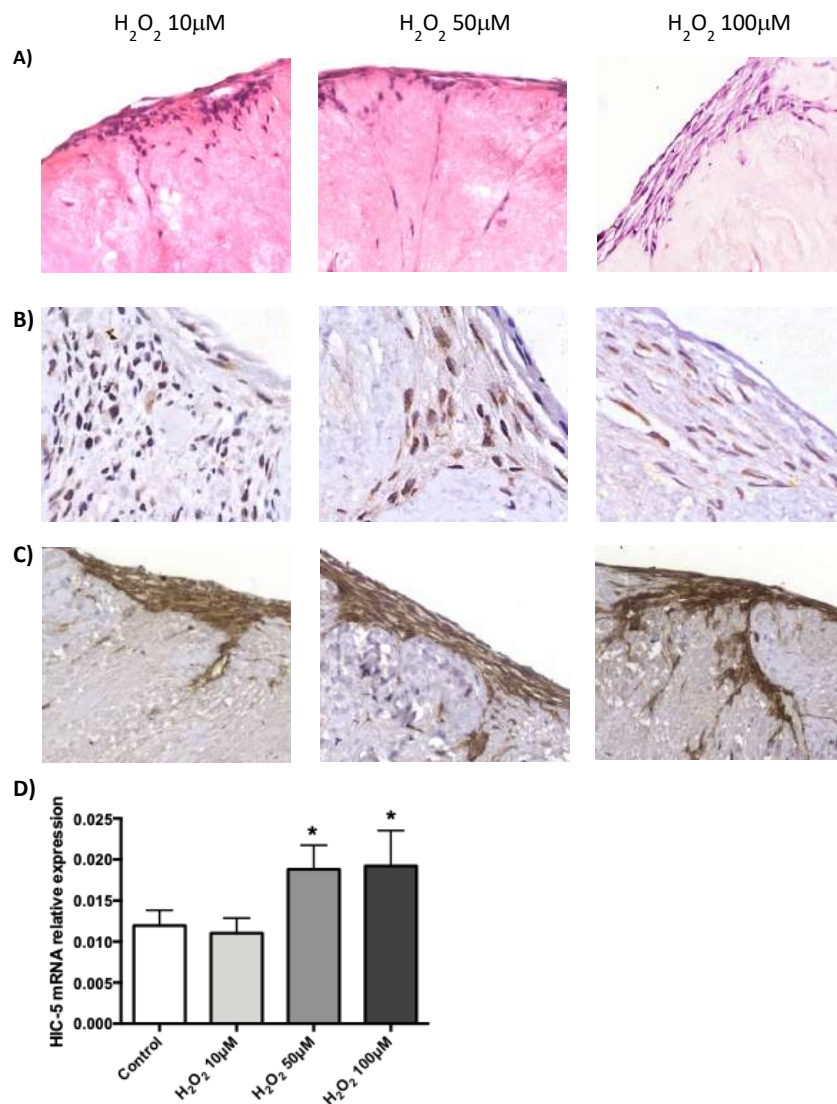


Figure 5. Treatment of primary human HSC cultured in healthy liver scaffolds with increasing concentration of hydrogen peroxide 5A) Haematoxylin and Eosin staining (40X magnification); 5B) Ki67 immunohistochemistry (100X magnification); 5C) PDGFβ receptor immunohistochemistry (40X magnification); 5D) Relative Hic-5 mRNA levels

assessed by qRT-PCR and normalized to GAPDH; n=5 per condition tested; mean and SD reported; * p<0.05, one-way ANOVA.

Hic-5 expression in HSC engrafting in healthy liver scaffolds was further confirmed by immunostaining (independent experiment, Fig.6).

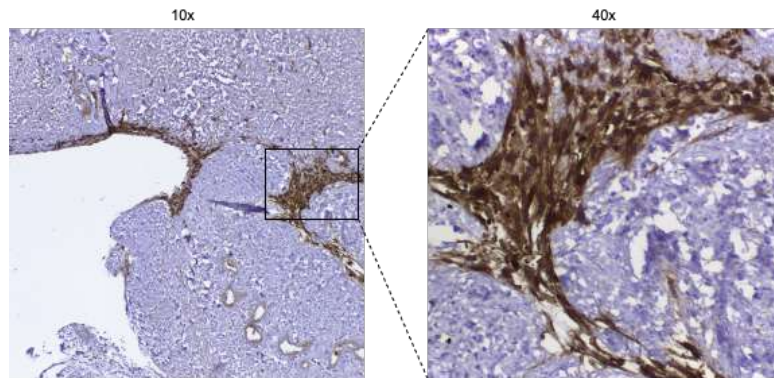


Figure 6. Representative images of Hic-5 immunohistochemistry showing Hic-5 positive HSC engrafting healthy liver scaffolds (10X and 40X magnification).

Hic-5 expression in primary human HSC: impact of liver ECM microenvironment.

The next question was whether change in hepatic ECM microenvironment could affect Hic-5 expression in human HSC. To address this issue, cells were cultured both in healthy and cirrhotic liver scaffolds and exposed to the following treatments: 1) H₂O₂ 100 μM for 24 h; 2) TGFβ1 5 ng/mL for 24 hours; 3) H₂O₂ 100 μM and TGFβ1 5ng/ml simultaneously for 24 hours; 4) H₂O₂ 100 μM or TGFβ1 5ng/ml pre-treatment for 6 hours followed by simultaneous treatment with H₂O₂ 100 μM and TGFβ1 5ng/ml for 18 hours.

PrestoBlue assay showed that cells remained viable in both type of ECM scaffolds with no significant difference among treatments, except in the group exposed to H₂O₂ 100 μM + TGFβ1 5ng/ml which showed a slight reduction in cell viability compared to the control in serum-free medium (Fig.7).

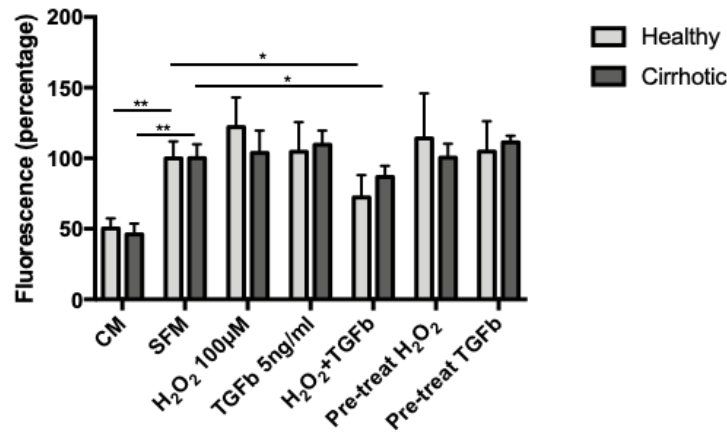


Figure 7. Human HSC remained viable both in healthy and cirrhotic scaffolds upon exposure to hydrogen peroxide/TGFβ. Cell viability was assessed by Prestoblue assay. Fluorescence data are reported as percentages compared to the control groups in serum-free medium (SFM) which were set at 100%. Data from H₂O₂+TGFβ group came from an independent experiment performed in parallel in healthy and cirrhotic scaffolds. CM= complete medium; N=5 per condition tested; mean and SD reported; * p<0.05; **p<0.01, one-way ANOVA.

Comparative gene expression analysis by qRT-PCR showed that HSC cultured in cirrhotic scaffolds expressed higher levels of Hic-5 mRNA compared to those in healthy scaffolds, suggesting that liver ECM itself can affect Hic-5 expression (Fig.8C). Interestingly, TGFβ induced Hic-5 gene expression in HSC cultured in healthy scaffolds (Fig.8A) but not in cirrhotic scaffolds (Fig.8B). To clarify whether this difference also involved other TGFβ target genes, ACTA2, COL1A1 and TGFβ1 mRNA levels were assessed in both 3D culture models. As shown in Fig.9, higher levels of COL1A1 were found in HSC cultured in cirrhotic scaffolds compared to healthy scaffolds, suggesting a greater activation of HSC by fibrotic ECM. A similar trend was observed for ACTA2 gene, although it did not reach statistical significance. Moreover, ACTA2, COL1A1 and TGFβ1 gene expression was increased by TGFβ exposure in HSC cultured in healthy scaffolds, while this effect was not observed in cirrhotic scaffolds, confirming that HSC respond to exogenous TGFβ differently, depending on the type of liver ECM i.e. healthy versus cirrhotic ECM.

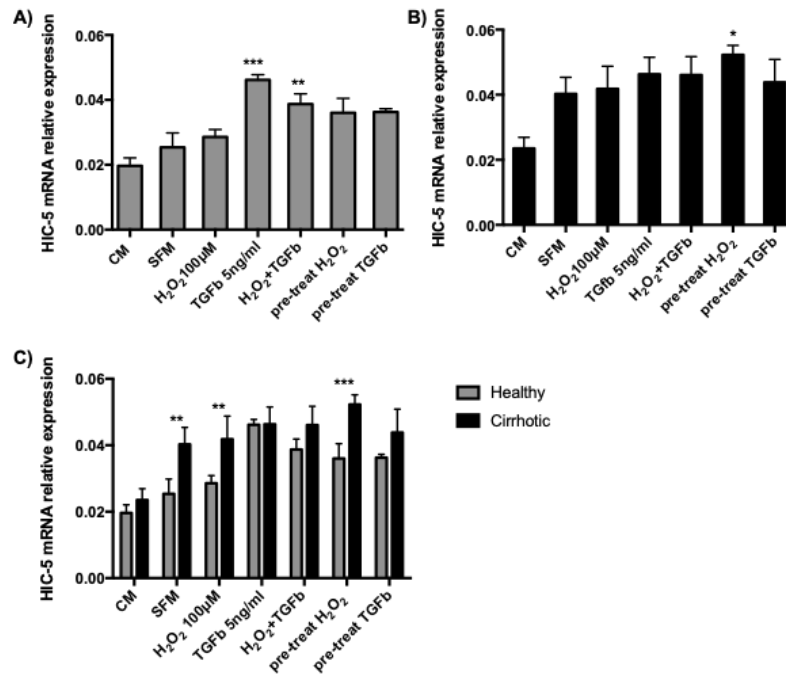


Figure 8. Hic-5 is differentially expressed by human HSC cultured in healthy and cirrhotic liver scaffolds.

Relative Hic-5 mRNA levels assessed by qRT-PCR and normalized to GAPDH. Data from H₂O₂+TGFβ group came from an independent experiment performed in parallel in healthy and cirrhotic scaffolds. N=4 per condition tested; mean and SD reported; CM= complete medium; SFM=serum-free medium* p<0.05, ** p<0.01, *** p<0.001, one-way ANOVA.

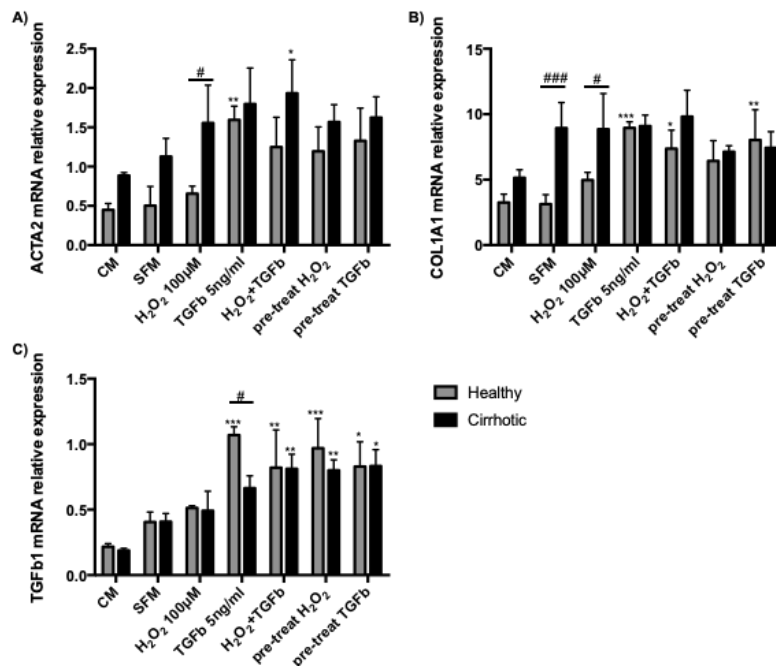


Figure 9. Liver ECM affects gene expression of activation markers in human HSC cultured in healthy and cirrhotic scaffolds.

Relative Hic-5 mRNA levels assessed by qRT-PCR and normalized to GAPDH. Data from H₂O₂+TGFβ group came from an independent experiment performed in parallel in healthy and cirrhotic scaffolds. N=4 per condition tested; mean and SD reported; CM= complete medium; SFM=serum-free medium; * p<0.05, ** p<0.01, *** p<0.001, one-way ANOVA.

The strong impact of liver ECM on HSC activation and response to fibrogenic stimuli was further confirmed by Western Blot analysis (Fig.10), showing higher levels of α -SMA in HSC cultured in cirrhotic scaffolds compared to healthy scaffolds. Furthermore, these preliminary data show no significant changes in Hic-5 protein expression when exposed singularly to H_2O_2 or TGF β in cells engrafting in 3D cirrhotic scaffolds, whereas simultaneous, or pretreatments induced a clear increase in Hic-5 protein expression in HSC engrafting cirrhotic 3D scaffolds compared to healthy scaffolds.

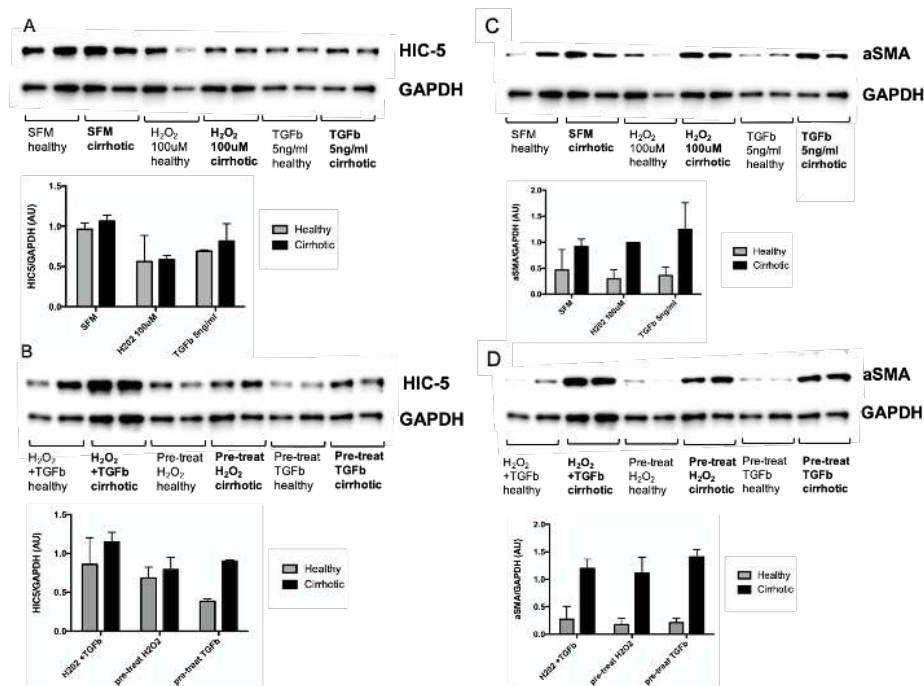


Figure 10. Hic-5 and α -SMA protein expression in HSC cultured in healthy and cirrhotic liver scaffolds. Western blot of Hic-5 (9A-B) and α -SMA (9C-D) expression and semiquantitative analysis showing protein expression normalized to GAPDH. N=2 per condition, mean and SD reported.

In summary, with this set of in-vitro experiments I investigated the expression of Hic-5 in primary human HSC cultured in a novel 3D-model based on human liver healthy and fibrotic ECM. These results demonstrate that Hic-5 expression in HSC is regulated by both TGF β and H_2O_2 and is strongly affected by hepatic ECM features, suggesting that its modulation could play a role in HSC activation. In order to further elucidate Hic-5 expression during hepatic fibrogenesis, I decided to focus my attention on NAFLD, a chronic liver disease caused by multiple pathological hits, including oxidative stress. Moreover, this model appears as the most appropriate to study the in vivo expression of Hic-5 since it is characterized by a wide spectrum of pathological findings, ranging from simple steatosis to steatohepatitis, fibrosis and ultimately cirrhosis.

Hic-5 is expressed in human NAFLD-induced liver fibrosis

The first step was to assess whether Hic-5 was expressed in human NAFLD. Human liver sections obtained from obese NASH patients undergoing bariatric surgery were stained for Hic-5. As shown in Fig. 10, a greater positivity was detected in the presence of moderate-severe fibrosis (Fig.11A), while very few positive cells were observed when mild fibrosis was diagnosed (Fig. 11B).

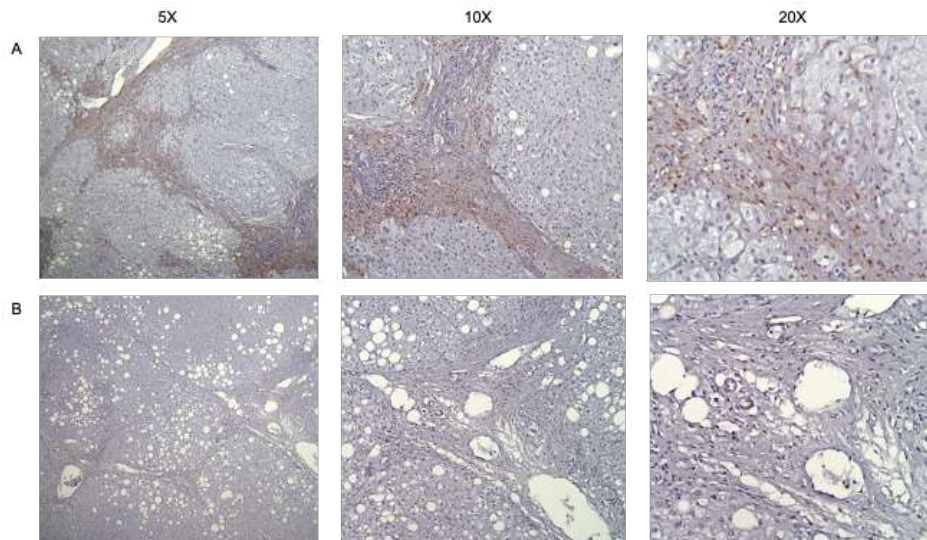


Figure 11. Microphotographs showing Hic-5 staining in human liver biopsies of NASH patients with either advanced (11A) or early fibrosis (11B).

Hic-5 positive cells were observed in the perisinusoidal spaces and along fibrotic septa (Fig.12A-B), whereas hepatocytes and inflammatory cells appeared negative (Fig 12C-D). Moreover Hic-5 expression overlapped with α -SMA positive areas, as shown by α -SMA staining. These results suggest that HSC are the main cells expressing Hic-5 in the setting of human NASH.

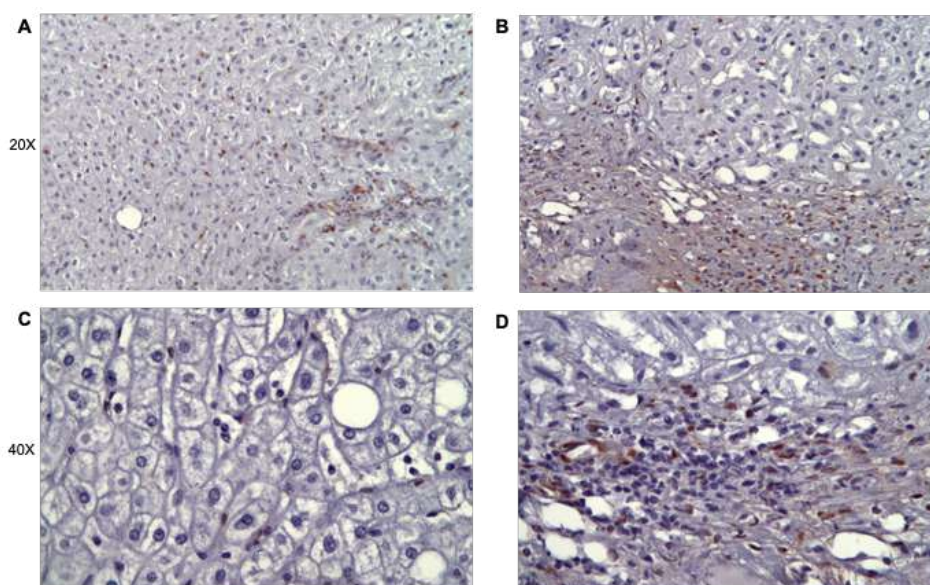


Figure 12. Hic-5 positive cells are located in the perisinusoidal spaces and along fibrotic septa in human NASH. Microphotographs of Hic-5 stained human livers (upper panels: 20X magnification; lower panels: 40X magnification).

Unfortunately, human liver samples are difficult to obtain in everyday clinical practice since liver biopsies are usually performed in a limited number of NAFLD patients, often presenting at advanced stage of disease. This limited availability precluded me to further investigate the relationship between Hic-5 expression and NAFLD progression in humans. Therefore, to overcome this limit, I decided to set up an experimental protocol, based on a nutritional rat model of NAFLD, able to recapitulate all the different stages of human disease.

Hic-5 is expressed during rat liver fibrogenesis

Since no data exist regarding Hic-5 expression in the setting of rat liver fibrogenesis, I first evaluate whether Hic-5 was induced in rat fibrotic liver. To this aim, I decided to employ the liver fibrosis model based on CCl₄ administration, since it is characterized by the rapid development of both liver fibrosis and hepatocyte necrosis and regeneration, as observed in the setting of human chronic hepatitis (63).

Hic-5 staining of liver sections obtained from rats administered CCl₄ for 9 weeks, revealed the presence of numerous Hic-5 positive cells, whose distribution matched α -SMA positive areas (Fig.13).

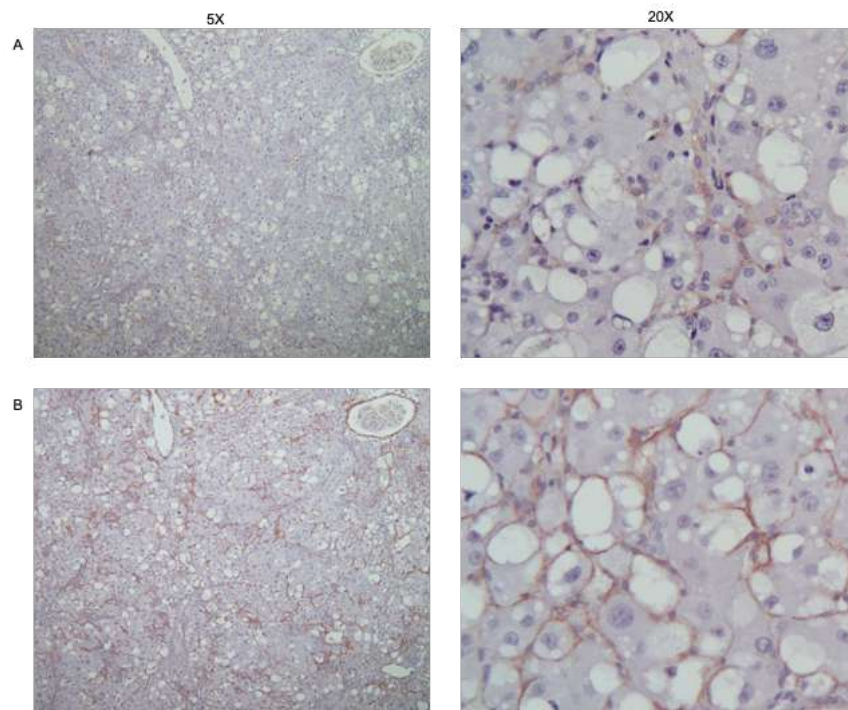


Figure 13. Hic-5 is expressed during rat liver fibrogenesis. Rat liver sections after 9 weeks of CCl₄ injections; A-B) Hic-5 immunohistochemistry staining C-D) Alfa-SMA immunohistochemistry (5X and 20x magnification).

Once demonstrated that a rat model can be used to study the *in vivo* expression of Hic-5 in the liver, my next step was to set up another experimental protocol which could allow me to dissect the molecular events that precede and support the development of liver fibrosis in the setting of steatohepatitis.

Hic-5 expression is not induced in rat fatty liver

I first decided to evaluate whether Hic-5 expression was associated to lipid accumulation in rat hepatocytes, independently of the presence of fibrosis. To test this hypothesis, I used an experimental model consisting of rats fed a CD diet for 3 days. This protocol was able to induce extensive steatosis with minimal signs of lobular inflammation and without any evidence of fibrosis. Immunostaining did not reveal any positivity for Hic-5 suggesting that simple steatosis did not induce Hic-5 expression in rat liver.

Gene expression analysis by qRT-PCR confirmed this finding, since no significant difference in Hic-5 mRNA levels was observed between rats fed CD or a CS diet for 3 days (Fig.14). Accordingly, Acta2 expression was unchanged.

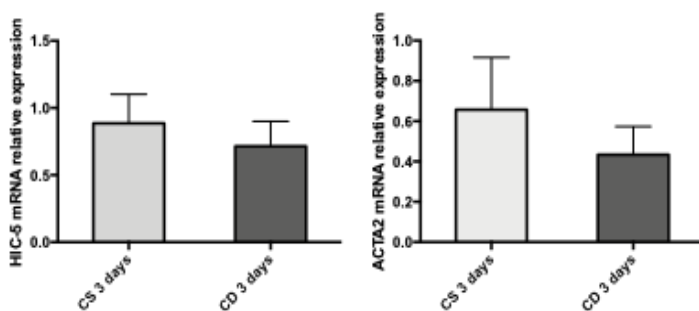


Figure 14. Hic-5 expression is not increased in rat fatty liver.

Relative Hic-5 and Acta2 mRNA levels assessed by qRT-PCR and normalized to GAPDH. N=7 per group, mean and SD reported.

Expression of Hic-5 in a rat model of NASH and its modulation by triiodothyronine-supplement diet

The next step was to investigate Hic-5 expression after 7 weeks of CD diet, a time point when steatosis is associated to lobular infiltration of inflammatory cells and perisinusoidal fibrosis, thus resembling the pathological findings of human NASH.

Hic-5 could be detected by immunohistochemistry, although the intensity of the staining was lower compared to alfa-SMA (Fig.15).

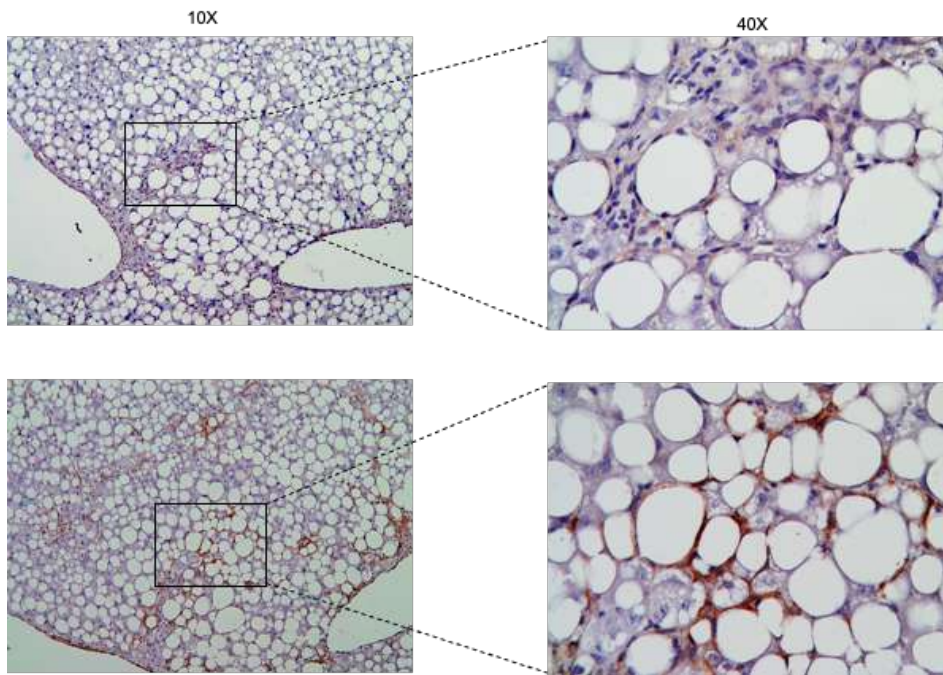


Figure 15. Representative images of Hic-5 (upper panels) and alpha-SMA (lower panels) stained rat liver from animals fed CD diet for 7 weeks (10 and 40X magnification).

Despite the weak immunostaining, a strong upregulation of Hic-5 gene expression was observed, along with other traditional HSC activation markers such as Acta2, Col1a1 and Tgfb1 (Fig.16).

Since targeting of hepatic thyroid hormone signaling pathways has been shown to produce beneficial effect in terms of NAFLD regression both in animal models and in humans (51,52), I decided to further investigate whether T3 administration could affect Hic-5 expression in rat liver.

As shown in Fig. 16, 1-week treatment with a T3-supplemented diet was able to reverse the induction of Hic-5, reducing gene expression back to control level. This effect was superior to that elicited by the switch from CD to CS diet. Moreover, a marked reduction in Acta2, Col1a1 and Tgfb1 mRNA levels was observed after T3-administration.

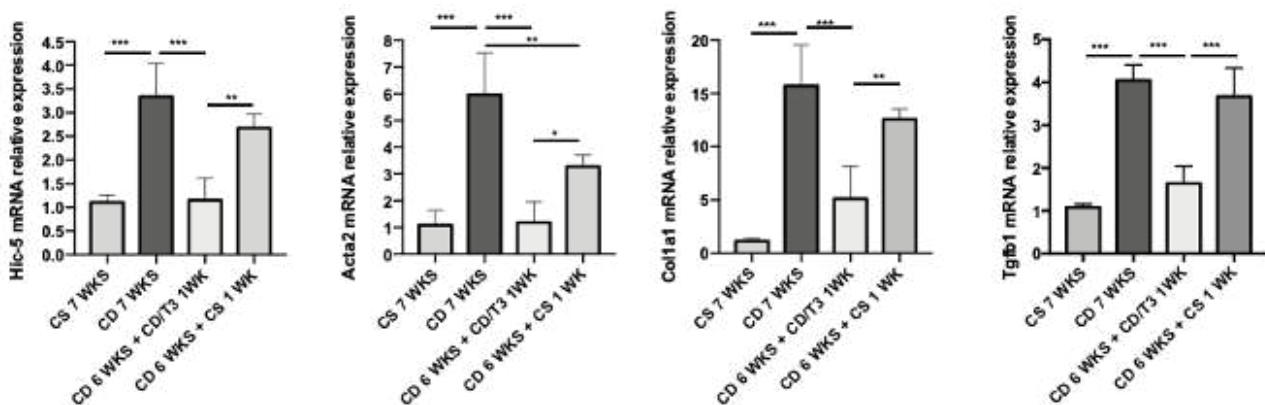


Figure 16. Relative mRNA levels of Hic-5, Acta-2, Col1a1 and Tgfb1 in the livers of rat fed CD diet for 7 weeks. GAPDH was used as endogenous control. N=5 per condition tested; mean and SD reported; CS: choline supplemented diet; CD: choline deficient diet; T3: triiodothyronine; * p<0.05, ** p<0.01, *** p<0.001, one-way ANOVA.

These findings were further confirmed at the protein level by Western Blot analysis (Fig.17).

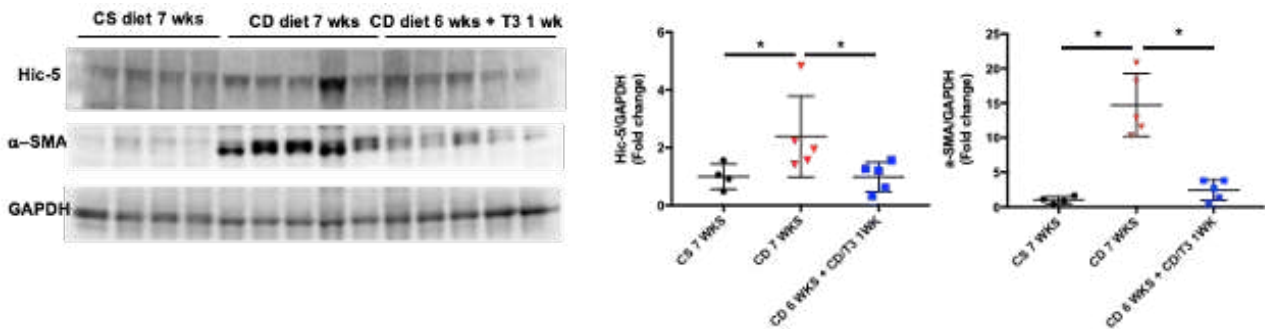


Figure 17. Western blot and semiquantitative analysis showing Hic-5 and α-SMA protein expression normalized to GAPDH. Mean and SD reported, * p<0.05.

Histological examination of rat liver sections stained with PicroSirius Red revealed a significant increase in the percentage of the collagen-positive area in animals fed the CD diet compared to CS diet (Fig.18). No significant difference was observed between CD diet and T3-treated animals.

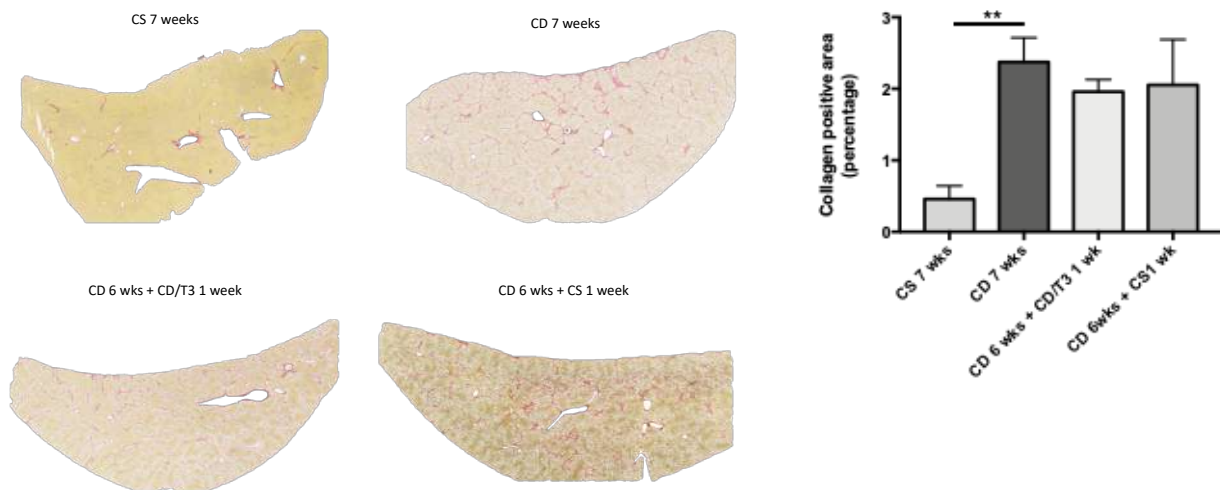


Figure 18. Representative images of PicroSirius red staining and quantitative analysis of collagen-positive area in rat liver sections. N=5 per group analyzed. ** p<0.01, one-way ANOVA.

Hic-5 is upregulated in a rat model of NAFLD-related hepatocarcinogenesis

Since NAFLD is a progressive liver disease which can ultimately lead to HCC development, my last step was to investigate whether Hic-5 upregulation could also be observed in NAFLD-related hepatocarcinogenesis. To this aim, I decided to employ another rat experimental protocol based on the administration of a single intraperitoneal dose of a well-known chemical carcinogen, namely DENA, followed by 11 weeks of CD diet. This model is able to induce the development of preneoplastic foci in the context of extensive steatohepatitis, recapitulating the histopathological features associated with human NAFLD progression to HCC (61). The 11-week time point was chosen

because it corresponded to a stage when only pre-neoplastic liver lesions could be detected. Therefore, it appeared to be the most appropriate for my studies since my aim was to dissect the molecular events that precedes or associates to the early phase of NAFLD-related hepatocarcinogenesis rather than those occurring in established HCC.

Based on this background, rats were injected intraperitoneally with a single dose of DENA and then fed a CD diet for 11 weeks. As shown in Fig.18, Hic-5 mRNA levels were strongly increased in the rats receiving DENA + CD diet compared to those receiving DENA + CS diet.

As already mentioned in the previous section, modulation of thyroid hormone signaling pathways by T3 and its analogs has been shown to have beneficial effect on NAFLD. Moreover, disruption of hepatic T3 signaling has been observed not only in human and experimental NAFLD, but also during hepatocarcinogenesis. In particular, a condition of local hepatic hypothyroidism has been shown to promote the progression of pre-neoplastic lesions to HCC in rats subjected to the Resistant-Hepatocyte model (64). Conversely, T3 treatment was able to induce the regression of rat pre-neoplastic GSTP-positive lesions induced by two different model of hepatocarcinogenesis (61).

Therefore, based on these previously published results, I wondered whether treatment with T3 could also affect Hic-5 expression in rats subjected to the DENA-CD model. As shown in Fig.19, administration of a T3-supplemented CD diet for 1 week was able to significantly decrease Hic-5 expression back to control levels. This effect was also observed on Acta2, Col1a1 and Tgfb1 gene expression. Interestingly, preneoplastic foci, identified by positive GSTP staining, did not show any Hic-5 accumulation, suggesting that the observed changes in mRNA levels did not occur inside the preneoplastic lesions, but in the surrounding parenchyma.

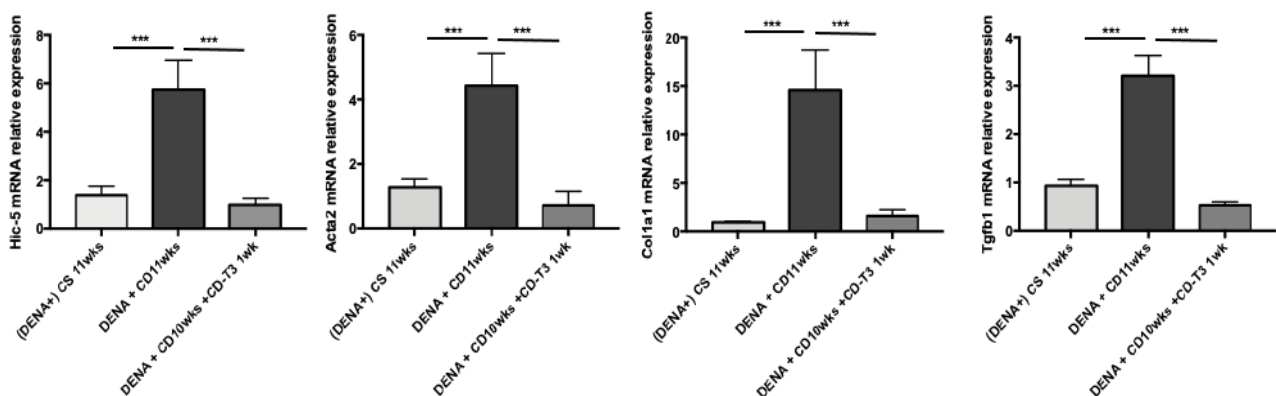


Figure 19. Relative mRNA levels of Hic-5, Acta2, Col1a1 and Tgfb1

GAPDH was used as endogenous control. N=5 per condition tested; mean and SD reported; DENA: diethylnitrosamine; CS: choline supplemented diet; CD: choline deficient diet; T3: triiodothyronine; * p<0.05, ** p<0.01, *** p<0.001, one-way ANOVA.

5. DISCUSSION

NAFLD represents one of the leading causes of chronic liver disease worldwide and is traditionally considered the hepatic manifestation of the metabolic syndrome. Fibrosis stage is the main determinant of liver-related mortality in NAFLD patients, therefore therapeutic strategies able to target both the metabolic alterations and the subsequent fibrosis development are urgently needed. Hic-5, a H₂O₂ and TGFβ-modulated protein, has recently been proposed as a novel therapeutic target for liver fibrosis, since its deficiency was shown to attenuate HSC activation in two mice models of liver fibrosis (33). So far, limited data exist on Hic-5 expression in human HSC and less is known regarding its role in NAFLD-induced liver fibrosis.

Based on this background, I investigated Hic-5 expression in primary HSC cultured in a novel 3D model based on healthy and fibrotic human liver ECM scaffolds. In contrast to traditional plastic cultures, this innovative system is able to mimic the 3D liver ECM microenvironment, which strongly affects HSC phenotype and response to pro-fibrogenic stimuli.

Hic-5 was significantly upregulated in HSC cultured in the 3D model compared to traditional 2D cultures, suggesting that its expression could be regulated by liver-specific ECM features. This observation is not surprising since Hic-5 has been found to locate at focal adhesions, which are complex multi-protein structures that mediate interactions between cells and ECM. Moreover, TGFβ exposure further increased Hic-5 expression in HSC cultured in healthy liver scaffolds, while this effect was not observed in the classical 2D model. Interestingly, HSC responded differently to TGFβ treatment depending on the type of liver scaffolds used (healthy versus cirrhotic).

As previously demonstrated, the cirrhotic liver scaffold matrix contains TGFβ1 and many TGFβ1 associated proteins with a significant retention of TGFβ1 specifically present in the cirrhotic ECM, which is released in the culture medium. Moreover, fibronectin (FN1), a major ECM protein and neo-epitope ECM marker of fibrogenesis, is a scavenger and a delivery system for the TGFβ1-LTBP1 complex and it is highly upregulated and secreted in the medium of cirrhotic scaffolds. Thus, the cirrhotic ECM is provided not only with a remarkable bioavailability of TGFβ1, but also with the necessary machinery for its activation in the tissue microenvironment. These data indicated that the cirrhotic scaffold has a unique and active ECM bio signature that could further affect the exogenous TGFβ1 effect on Hic-5 expression in HSC cultured in cirrhotic ECM scaffolds (44).

Starting from these preliminary results obtained in the in-vitro model, I decided to further investigate the role of Hic-5 in liver fibrogenesis, focusing my interest on NAFLD-induced fibrosis. This condition is known to be driven by oxidative stress and inflammation, which are associated with

high TGF β levels and subsequent strong HSC activation (65). Immunostaining of human liver sections obtained from obese NASH patients revealed that Hic-5 was strongly expressed in the perisinusoidal spaces and fibrotic septa in the presence of moderate-severe fibrosis. Conversely, its expression was nearly absent in case of mild fibrosis. These findings documented for the first time the expression of Hic-5 in human NAFLD and further supported its role in human liver fibrogenesis.

To better elucidate the role of Hic-5 along NAFLD progression, I decided to employ a well-established rat model of NAFLD, based on the administration of a choline-deficient (CD) diet, which is able to recapitulate all the different stages of human disease. This model also allowed to study whether the stimulation of the thyroid hormone signaling, a novel therapeutic strategy that is under clinical evaluation for NAFLD, could affect Hic-5 expression and NAFLD-induced fibrosis.

Using the in-vivo model of NAFLD, I could demonstrate that Hic-5 expression was not induced in rat fatty liver when at early stages hepatic steatosis is not associated with significant inflammatory and fibrotic response. This observation further supports the hypothesis that, in the context of NAFLD, Hic-5 has to be considered a marker of liver fibrosis rather than fatty liver itself. In contrast, Hic-5 was strongly upregulated in the setting of NASH, along with other traditional HSC activation markers, such as α -SMA and Col1a1. Interestingly, treatment with a T3-supplemented diet was able to reverse this induction, although this effect was not associated with a concomitant decrease in liver fibrosis.

Unfortunately, I could not investigate whether this downregulation was due to a direct modulation of Hic-5 expression by T3 in HSC or it was the consequence of the beneficial metabolic impact of T3 treatment in NAFLD and the subsequent reduction in HSC activation and fibrogenesis. Interestingly, T3 binding to its nuclear receptors has been shown to inhibit TGF β signaling in a cell line of mink epithelial cells through a direct interaction with SMAD3 and SMAD4, a reduced SMAD phosphorylation and a decreased SMAD recruitment to TGF β target gene promoters (57). So far, there are no published data regarding a direct regulation of Hic-5 by thyroid hormone, neither in HSC nor in other cells, therefore this issue deserves to be further investigated in future studies.

These results show that even in the carcinogenesis model T3 regulates the expression of Hic-5. However, these experiments do not unveil the contribution of Hic-5 on the progression of the carcinogenesis process. Indeed, in this experiment it was not possible to assess whether the inhibition of Hic-5 expression precedes the disappearance of the preneoplastic lesions or is an independent effect mediated by T3. It also remains to be shown whether preneoplastic hepatocytes express Hic-5. In fact, the immunohistochemical technique is not sensitive enough to detect a low

expression of the protein. For this, the next step will be to evaluate the expression of Hic-5 by qPCR assay on preneoplastic lesions, which will be microdissected by laser-assisted technique. These results will be relevant considering that recently published studies have highlighted a potential role of Hic-5 in different tumors, including HCC. In particular, Hic-5 has been proposed as a prognostic marker in HCC progression, since a greater Hic-5 expression was reported in patient-derived HCC cells with high motility and in subjects with intra and extrahepatic metastasis (66). Therefore, to further clarify this issue, specific analysis from dissected pre-neoplastic nodules will be performed to better investigate Hic-5 expression during the early phases of hepatocarcinogenesis.

Taken altogether, the results obtained in the present project contribute to further understand the mechanisms underlying Hic-5 expression in the context of NAFLD, providing the basis for future studies focusing on the identification of novel anti-fibrotic strategies.

References

1. Marchesini G, Day CP, Dufour JF, Canbay A, Nobili V, Ratziu V, et al. EASL-EASD-EASO Clinical Practice Guidelines for the management of non-alcoholic fatty liver disease. *J Hepatol*. 2016; 64(6):1388-1402.
2. Ludwig J, Viggiano TR, McGill DB, Oh BJ. Nonalcoholic steatohepatitis: Mayo Clinic experiences with a hitherto unnamed disease. *Mayo Clin Proc*. 1980 Jul;55(7):434–8.
3. Younossi ZM, Koenig AB, Abdelatif D, Fazel Y, Henry L, Wymer M. Global epidemiology of nonalcoholic fatty liver disease—Meta-analytic assessment of prevalence, incidence, and outcomes. *Hepatology*. 2016;64(1):73-84.
4. Estes C, Anstee QM, Arias-Loste MT, Bantel H, Bellentani S, Caballeria J, et al. Modeling NAFLD disease burden in China, France, Germany, Italy, Japan, Spain, United Kingdom, and United States for the period 2016–2030. *J Hepatol*. 2018; 69(4):896-904.
5. Wong RJ, Aguilar M, Cheung R, Perumpail RB, Harrison SA, Younossi ZM, et al. Nonalcoholic steatohepatitis is the second leading etiology of liver disease among adults awaiting liver transplantation in the United States. *Gastroenterology*. 2015; 148(3):547-55.
6. Younossi ZM, Otgonsuren M, Henry L, Venkatesan C, Mishra A, Erario M, et al. Association of nonalcoholic fatty liver disease (NAFLD) with hepatocellular carcinoma (HCC) in the United States from 2004 to 2009. *Hepatology*. 2015; 62(6):1723-30.
7. Anstee QM, Targher G, Day CP. Progression of NAFLD to diabetes mellitus, cardiovascular disease or cirrhosis. *Nat Rev Gastroenterol Hepatol*. 2013;10(6):330–44.
8. Bellentani S, Bedogni G, Miglioli L, Tiribelli C. The epidemiology of fatty liver. *Eur J Gastroenterol Hepatol* 2004; 16(11):1087-93.
9. Sookoian S, Castaño GO, Burgueño AL, Gianotti TF, Rosselli MS, Pirola CJ. A nonsynonymous gene variant in the adiponutrin gene is associated with nonalcoholic fatty liver disease severity. *J Lipid Res*. 2009; 50(10):2111–6.
10. Rotman Y, Koh C, Zmuda JM, Kleiner DE, Liang TJ. The association of genetic variability in patatin-like phospholipase domain-containing protein 3 (PNPLA3) with histological severity of nonalcoholic fatty liver disease. *Hepatology*. 2010; 52(3):894–903.
11. Singal AG, Manjunath H, Yopp AC, Beg MS, Marrero JA, Gopal P, et al. The effect of PNPLA3 on fibrosis progression and development of hepatocellular carcinoma: a meta-analysis. *Am J Gastroenterol*. 2014; 109(3):325–34.
12. Teli MR, James OF, Burt AD, Bennett MK, Day CP. The natural history of nonalcoholic fatty liver: a follow-up study. *Hepatology*. 1995; 22(6):1714–9.
13. Söderberg C, Stål P, Askling J, Glaumann H, Lindberg G, Marmur J, et al. Decreased survival of subjects with elevated liver function tests during a 28-year follow-up. *Hepatology*. 2010; 51(2):595–602.
14. Singh S, Allen AM, Wang Z, Prokop LJ, Murad MH, Loomba R. Fibrosis Progression in Nonalcoholic Fatty Liver vs Nonalcoholic Steatohepatitis: A Systematic Review and Meta-analysis of Paired-Biopsy Studies. *Clin Gastroenterol Hepatol*. 2015; 13(4):643-54.e1-9
15. Torres DM, Williams CD, Harrison SA. Features, Diagnosis, and Treatment of Nonalcoholic Fatty Liver Disease. *Clin Gastroenterol Hepatol* 2012; 10(8):837-58.
16. Mittal S, El-Serag HB, Sada YH, Kanwal F, Duan Z, Temple S, et al. Hepatocellular Carcinoma in the Absence of Cirrhosis in United States Veterans is Associated With Nonalcoholic Fatty Liver Disease. *Clin Gastroenterol*

- Hepatology 2016; 46(1):124-31.
17. Dyson J, Jaques B, Chattopadhyay D, Lochan R, Graham J, Das D, et al. Hepatocellular cancer: The impact of obesity, type 2 diabetes and a multidisciplinary team. *J Hepatol* 2014; 60(1):110–7.
 18. Piscaglia F, Svegliati-Baroni G, Barchetti A, Pecorelli A, Marinelli S, Tiribelli C, et al. Clinical patterns of hepatocellular carcinoma in nonalcoholic fatty liver disease: A multicenter prospective study. *Hepatology*. 2016; 63(3):827–38.
 19. Day CP, James OF. Steatohepatitis: a tale of two “hits”? *Gastroenterology* 1998; 114(4):842–5.
 20. Buzzetti E, Pinzani M, Tsochatzis EA. The multiple-hit pathogenesis of non-alcoholic fatty liver disease (NAFLD). *Metabolism* 2016; 65(8):1038-48.
 21. Cusi K. Role of insulin resistance and lipotoxicity in non-alcoholic steatohepatitis. *Clin Liver Dis*. 2009; 13(4):545–63.
 22. Guilherme A, Virbasius J V, Puri V, Czech MP. Adipocyte dysfunctions linking obesity to insulin resistance and type 2 diabetes. *Nat Rev Mol Cell Biol*. 2008; 9(5):367–77.
 23. Kirpich IA, Marsano LS, McClain CJ. Gut-liver axis, nutrition, and non-alcoholic fatty liver disease. *Clin Biochem*. 2015;48(13–14):923–30.
 24. Kim KH, Lee M-S. Pathogenesis of Nonalcoholic Steatohepatitis and Hormone-Based Therapeutic Approaches. *Front Endocrinol (Lausanne)*. 2018;9:485.
 25. Angulo P, Kleiner DE, Dam-Larsen S, Adams LA, Bjornsson ES, Charatcharoenwitthaya P, et al. Liver Fibrosis, but No Other Histologic Features, Is Associated With Long-term Outcomes of Patients With Nonalcoholic Fatty Liver Disease. *Gastroenterology*. 2015; 149(2):389-97.e10.
 26. Vilar-Gomez E, Calzadilla-Bertot L, Wai-Sun Wong V, Castellanos M, Aller-de la Fuente R, Metwally M, et al. Fibrosis Severity as a Determinant of Cause-Specific Mortality in Patients With Advanced Nonalcoholic Fatty Liver Disease: A Multi-National Cohort Study. *Gastroenterology*. 2018; 155(2):443-457.e17.
 27. Ni Y, Li JM, Liu MK, Zhang TT, Wang DP, Zhou WH, et al. Pathological process of liver sinusoidal endothelial cells in liver diseases. *World J Gastroenterol*. 2017; 23(43):7666-77.
 28. Mederacke I, Hsu CC, Troeger JS, Huebener P, Mu X, Dapito DH, et al. Fate tracing reveals hepatic stellate cells as dominant contributors to liver fibrosis independent of its aetiology. *Nat Commun*. 2013; 4:2823.
 29. Tsuchida T, Friedman SL. Mechanisms of hepatic stellate cell activation. *Nat Rev Gastroenterol Hepatol*. 2017; 14(7):397-411.
 30. Schon H-T, Weiskirchen R. Immunomodulatory effects of transforming growth factor- β in the liver. *Hepatobiliary Surg Nutr*. 2014; 3(6):386–406.
 31. Robertson IB, Rifkin DB. Regulation of the Bioavailability of TGF- β and TGF- β -Related Proteins. *Cold Spring Harb Perspect Biol*. 2016; 8(6):a021907.
 32. Henderson NC, Arnold TD, Katamura Y, Giacomini MM, Rodriguez JD, McCarty JH, et al. Targeting of αv integrin identifies a core molecular pathway that regulates fibrosis in several organs. *Nat Med*. 2013; 19(12):1617–24.
 33. Lei XF, Fu W, Kim-Kaneyama JR, Omoto T, Miyazaki T, Li B, et al. Hic-5 deficiency attenuates the activation of hepatic stellate cells and liver fibrosis through upregulation of Smad7 in mice. *J Hepatol*. 2016; 64(1):110-7.
 34. Shibamura M, Mashimo JI, Kuroki T, Nose K. Characterization of the TGF β 1-inducible Hic-5 gene that encodes a putative novel zinc finger protein and its possible involvement in cellular senescence. *J Biol Chem*. 1994;

269(43):26767-74.

35. Kim-Kaneyama J, Suzuki W, Ichikawa K, Ohki T, Kohno Y, Sata M, et al. Uni-axial stretching regulates intracellular localization of Hic-5 expressed in smooth-muscle cells in vivo. *J Cell Sci.* 2005 ;118(5):937-949.
36. Petit V, Thiery JP. Focal adhesions: Structure and dynamics. *Biol Cell.* 2000; 92(7):477-94.
37. Kim-Kaneyama J, Lei XF, Arita S, Miyauchi A, Miyazaki T, Miyazaki A. Hydrogen peroxide-inducible clone 5 (Hic-5) as a potential therapeutic target for vascular and other disorders. *Journal of Atherosclerosis and Thrombosis.* 2012; 19(7):601-607.
38. Wang H, Song K, Krebs TL, Yang J, Danielpour D. Smad7 is inactivated through a direct physical interaction with the LIM protein Hic-5/ARA55. *Oncogene* 2008; 27, 6791–6805.
39. Dabiri G, Tumbarello DA, Turner CE, Van de Water L. Hic-5 promotes the hypertrophic scar myofibroblast phenotype by regulating the TGF-beta1 autocrine loop. *J Invest Dermatol* 2008; 128(10):2518–25.
40. Hornigold N, Craven RA, Keen JN, Johnson T, Banks RE, Mooney AF. Upregulation of Hic-5 in glomerulosclerosis and its regulation of mesangial cell apoptosis. *Kidney Int.* 2010; 77(4) 329-338.
41. Paul J, Singh AK, Kathania M, Elviche TL, Zeng M, Basrur V, et al. IL-17-driven intestinal fibrosis is inhibited by Itch-mediated ubiquitination of Hic-5. *Mucosal Immunol.* 2018; 11, 427–436.
42. Gao L, Lei X-F, Miyauchi A, Noguchi M, Omoto T, Haraguchi S, et al. Hic-5 is required for activation of pancreatic stellate cells and development of pancreatic fibrosis in chronic pancreatitis. *Sci Rep.* 2020; 10(1):19105.
43. Piera-Velazquez S, Fertala J, Huaman-Vargas G, Louneva N, Jiménez SA. Increased expression of the transforming growth factor β -inducible gene Hic-5 in systemic sclerosis skin and fibroblasts: a novel antifibrotic therapeutic target. *Rheumatology (Oxford).* 2020; 59(10):3092–8.
44. Mazza G, Telese A, Al-Akkad W, Frenguelli L, Levi A, Marrali M, et al. Cirrhotic Human Liver Extracellular Matrix 3D Scaffolds Promote Smad-Dependent TGF- β 1 Epithelial Mesenchymal Transition. *Cells.* 2019 Dec;9(1): 83.
45. Ritter MJ, Amano I, Hollenberg AN. Thyroid Hormone Signaling and the Liver. *Hepatology* 2020;72(2):742–52.
46. Mantovani A, Nascimbeni F, Lonardo A, Zoppini G, Bonora E, Mantzoros CS, et al. Association Between Primary Hypothyroidism and Nonalcoholic Fatty Liver Disease: A Systematic Review and Meta-Analysis. *Thyroid* 2018;28(10):1270–84.
47. Guo Z, Li M, Han B, Qi X. Association of non-alcoholic fatty liver disease with thyroid function: A systematic review and meta-analysis. *Dig liver Dis Off J Ital Soc Gastroenterol Ital Assoc Study Liver* 2018;50(11):1153–62.
48. Pihlajamäki J, Boes T, Kim E-Y, Dearie F, Kim BW, Schroeder J, et al. Thyroid Hormone-Related Regulation of Gene Expression in Human Fatty Liver. *J Clin Endocrinol Metab* 2009; 94(9):3521–9.
49. Bohinc BN, Michelotti G, Xie G, Pang H, Suzuki A, Guy CD, et al. Repair-related activation of hedgehog signaling in stromal cells promotes intrahepatic hypothyroidism. *Endocrinology* 2014; 155(11):4591–601.
50. Krause C, Grohs M, El Gammal AT, Wolter S, Lehnert H, Mann O, et al. Reduced expression of thyroid hormone receptor β in human nonalcoholic steatohepatitis. *Endocr Connect.* 2018; 7(12):1448–56.
51. Perra A, Simbula G, Simbula M, Pibiri M, Kowalik MA, Sulas P, et al. Thyroid hormone (T3) and TR β agonist GC-1 inhibit/reverse nonalcoholic fatty liver in rats. *FASEB J.* 2008; 22(8):2981-9.
52. Harrison SA, Bashir MR, Guy CD, Zhou R, Moylan CA, Frias JP, et al. Resmetirom (MGL-3196) for the treatment of non-alcoholic steatohepatitis: a multicentre, randomised, double-blind, placebo-controlled, phase 2 trial. *Lancet* 2019; 394(10213):2012-24.

53. Loomba R, Neutel J, Mohseni R, Bernard D, Severance R, Dao M, et al. LBP-20-VK2809, a Novel Liver-Directed Thyroid Receptor Beta Agonist, Significantly Reduces Liver Fat with Both Low and High Doses in Patients with Non-Alcoholic Fatty Liver Disease: A Phase 2 Randomized, Placebo-Controlled Trial. *J Hepatol* 2019; 70(1):e150–1.
54. Lisssoos TW, Beno DWA, Davis BH. Posttranslational inhibition of Ito cell type I collagen production by triiodothyronine. *Am J Physiol - Gastrointest Liver Physiol.* 1993; 264(6 Pt 1):G1090-5.
55. Zvibel I, Atias D, Phillips A, Halpern Z, Oren R. Thyroid hormones induce activation of rat hepatic stellate cells through increased expression of p75 neurotrophin receptor and direct activation of Rho. *Lab Investig.* 2010; 90, 674–684.
56. Kariv R, Enden A, Zvibel I, Rosner G, Brill S, Shafritz DA, et al. Triiodothyronine and interleukin-6 (IL-6) induce expression of HGF in an immortalized rat hepatic stellate cell line. *Liver Int.* 2003; 23(3):187-93.
57. Alonso-Merino E, Orozco RM, Ruíz-Llorente L, Martínez-Iglesias OA, Velasco-Martín JP, Montero-Pedrazuela A, et al. Thyroid hormones inhibit TGF- β signaling and attenuate fibrotic responses. *Proc Natl Acad Sci U S A.* 2016; 113(24):E3451-60.
58. Longato L, Andreola F, Davies SS, Roberts JL, Fusai G, Pinzani M, et al. Reactive gamma-ketoaldehydes as novel activators of hepatic stellate cells in vitro. *Free Radic Biol Med.* 2017; 102:162-173.
59. Rombouts K, Carloni V. Determination and characterization of tetraspanin- Associated phosphoinositide-4 kinases in primary and neoplastic liver cells. *Methods Mol Biol.* 2016; 1376:203-12.
60. Mazza G, Al-Akkad W, Telese A, Longato L, Urbani L, Robinson B, et al. Rapid production of human liver scaffolds for functional tissue engineering by high shear stress oscillation-decellularization. *Sci Rep.* 2017;7: 5534.
61. Perra A, Kowalik MA, Pibiri M, Ledda-Columbano GM, Columbano A. Thyroid hormone receptor ligands induce regression of rat preneoplastic liver lesions causing their reversion to a differentiated phenotype. *Hepatology* 2009; 49(4):1287–96.
62. Shinozuka, H., Lombardi, B., Sell, S., and Iammarino, R. M. Early histological and functional alterations of ethionine liver carcinogenesis in rats fed a choline-deficient diet. *Cancer Res.* 1978; 38 (4): 1092–98.
63. Pérez Tamayo R. Is cirrhosis of the liver experimentally produced by CCl₄ and adequate model of human cirrhosis? *Hepatology* 1983;3(1):112-20.
64. Frau C, Loi R, Petrelli A, Perra A, Menegon S, Kowalik MA, et al.. Local hypothyroidism favors the progression of preneoplastic lesions to hepatocellular carcinoma in rats. *Hepatology* 2015;61(1):249-59.
65. Nair B, Nath LR. Inevitable role of TGF- β 1 in progression of nonalcoholic fatty liver disease. *J Recept Signal Transduct Res.* 2020; 40(3):195–200.